Journal of the OPTICAL SOCIETY *of* AMERICA

VOLUME 25
No. 11

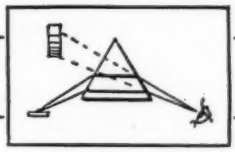

NOVEMBER
1935

Dispersion of CS_2 and CCl_4 in the Infrared . . . . . A. H. PFUND 351

Absorption Tube for the Investigation of Gases in the Photographic Infrared . . RICHARD M. BADGER, LYMAN G. BONNER AND PAUL C. CROSS 355

Polarization-Interference Phenomena in Quartz Spectrographs . . . . . JOSEPH W. ELLIS AND JOSEPH KAPLAN 357

Maximum Visual Efficiency of Colored Materials . . . DAVID L. MACADAM 361

Luminescence of Frozen Solutions of Certain Dyes . . . . . FRANCES G. WICK AND CHARLOTTE G. THROOP 368

Simple Stroboscope . . . . . AUSTIN J. O'LEARY 375

Published monthly
at Prince and Lemon Sts., Lancaster, Pa.
by the
AMERICAN INSTITUTE OF PHYSICS
Incorporated
11 East 38th Street, New York, N. Y.
FOR AND UNDER THE EDITORIAL SUPERVISION OF
THE OPTICAL SOCIETY OF AMERICA

THE OPTICAL SOCIETY OF AMERICA

OFFICERS OF THE SOCIETY

W. B. RAYTON, *President*
Bausch & Lomb Optical Company
Rochester, New York

ARTHUR C. HARDY, *Vice President*
Massachusetts Institute of Technology
Cambridge, Massachusetts

L. B. TUCKERMAN, *Secretary*
Bureau of Standards
Washington, D. C.

HENRY F. KURTZ, *Treasurer*
Bausch & Lomb Optical Company
Rochester, New York

The Board of Directors consists of the above officers; the Editor of the Journal; the Past President; and five elected members:

E. C. CRITTENDEN, *Past President*
Bureau of Standards
Washington, D. C.

F. K. RICHTMYER, *Editor*
Cornell University
Ithaca, New York

Elected Members

ARTHUR H. COMPTON
Ryerson Physical Laboratory
University of Chicago
Chicago, Illinois

HERBERT E. IVES
463 West Street
New York, New York

CARL W. KEUFFEL
Keuffel & Esser Company
Hoboken, New Jersey

GEORGE B. PEGRAM
Columbia University
New York, New York

R. C. GIBBS
Department of Physics
Cornell University
Ithaca, New York

THE OPTICAL SOCIETY OF AMERICA was organized in 1916 "*to increase and diffuse the knowledge of optics in all its branches, pure and applied, to promote the mutual interests of investigators of optical problems, of designers, manufacturers and users of optical instruments and apparatus of all kinds and to encourage cooperation among them.*" It aims to serve the interests of all who are engaged in any branch of optics from fundamental research to the manufacture of optical goods.

MEMBERSHIP

Regular Members: "Any person who has contributed materially to the advancement of optics is eligible for regular membership."

Associate Members: "Any person who is interested in optics is eligible for associate membership."

Corporate Members: "Any corporation desirous of encouraging the work of the Society is eligible for corporation membership."

The Society cordially invites to membership all who are interested in any branch of optics, either in research, in instruction, in optical or illuminating engineering, in the manufacture and distribution of optical goods of all kinds or in physiological and medical optics.

ANNUAL DUES

Regular members, $7.50; Associate members, $5.00; Corporate members, $50.00. These dues include subscription to the Society's official journal, the *Journal of the Optical Society of America.*

MEETINGS

The Society holds two meetings per year: An annual meeting in the autumn and a midwinter meeting jointly with the American Physical Society.

For further information concerning the Optical Society of America address the Secretary, Dr. L. B. Tuckerman, Bureau of Standards, Washington, D. C.

ROCHESTER, NEW YORK SECTION OF THE OPTICAL SOCIETY OF AMERICA

C. C. NITCHIE, *President*
H. E. SEEMANN, *Secretary*

L. A. DUBRIDGE, *Vice President*
H. G. KINGSLAKE, *Treasurer*

Councilors: E. C. FRITTS, R. KINGSLAKE, H. F. KURTZ, T. R. WILKINS, C. J. STAUD (*ex-officio*)

Journal of the
OPTICAL SOCIETY
of AMERICA

VOLUME 25 NOVEMBER, 1935 NUMBER 11

The Dispersion of CS_2 and CCl_4 in the Infrared

A. H. PFUND, *Johns Hopkins University*
(Received August 15, 1935)

THE purpose of this investigation is to present data on the dispersion and absorption of the two most highly transparent liquids in the infrared. It is proposed to use this information for the purpose of extending to regions of greater wave-length the quantitative test of Rayleigh's law of scattering.[1] In addition, the determinations of the wave-lengths of the several absorption bands will make possible a test of dispersion formulae over a wide range of frequencies. Finally, the results obtained find application in the discussion of "transition probabilities."

The only information on the dispersion of liquids in the infrared is that due to Rubens.[2] His work on carbon bisulphide, xylol and benzene was carried out with hollow prisms having glass sides. Because of the opacity of the glass, measurements could be carried out only to 2μ. Rubens found that the course of the dispersion curves followed that of the simple Cauchy dispersion formula.

In the present study, hollow prisms with sides of polished rocksalt were employed and in consequence, the wave-length range could be increased considerably. For purposes of orientation preliminary measurements were made with a glass-sided prism having the relatively large angle of 38° 1′; these were followed by measurements with an acute angled prism with rocksalt sides. The angle of this prism (15° 23′ 24″) was purposely made small so as to make possible the exploration of dispersion into the regions of large absorption. Unfortunately, the rocksalt plates had to be polished by hand; though moderately plane-parallel, they always showed curvature near the edges. Since the thinnest portion of the prism is the most valuable, it is evident that here the rocksalt plates would be the most defective. This difficulty was minimized by procuring a plate of double the desired size, polishing it and breaking it in two along a central line where the figure is best. The broken edges were then made to meet at the apex of the prism. The plates (3×4 cm) were attached to the brass frame with nitrocellulose dissolved in amyl acetate; later, shellac in alcohol was painted around the edges.

The apparatus consisted of two mirror spectrometers in series: the first, illuminated by a Nernst lamp and with a rocksalt prism, served as a monochromator for the second which contained the hollow prism filled with the liquid under consideration. Both spectrometers were equipped with Wadsworth mirrors; all concave mirrors were of 30 cm focal length; all three slits were 0.3 mm wide. Since the spectrometers are of the conventional type and, since the procedure is obvious, a detailed description is unnecessary. It may be stated, however, that even with the 15° prism refractive indices were measured to a

[1] A. H. Pfund, J. O. S. A. **24**, 143 (1934).
[2] H. Rubens, Ann. d. Physik **45**, 238 (1892).

BOSTON UNIVERSITY
COLLEGE OF LIBERAL ARTS
LIBRARY

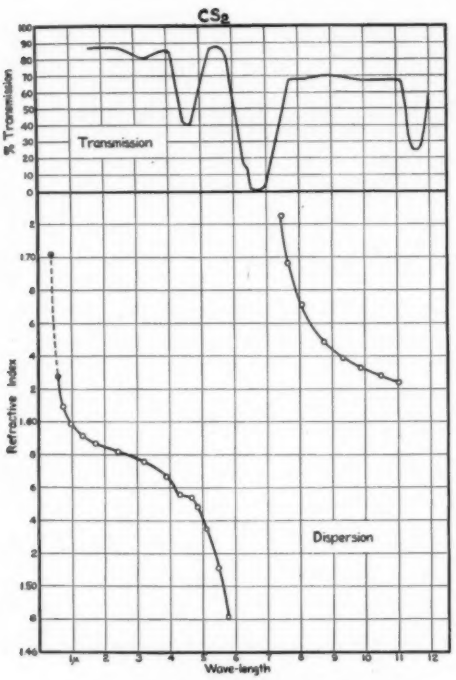

FIG. 1. Dispersion of carbon disulphide.

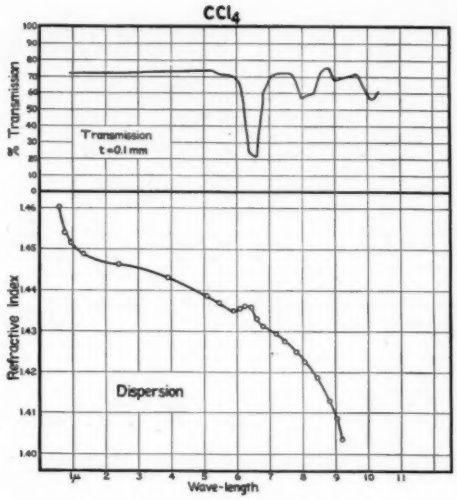

FIG. 2. Dispersion of carbon tetrachloride.

reproducible accuracy of ± 0.0004. Because of the uncertainties introduced by the rocksalt plates the absolute accuracy is held to be no better than one or two units in the third decimal place.

The thermocouple, which was of the usual single-junction type, was mounted in a glass cell containing P_2O_5. Before evacuation, a little CCl_4 was poured over the glass wool holding the P_2O_5 in place and the vapors were allowed to diffuse for about five minutes. The system was then connected to an old oil-pump which was kept in operation for about ten minutes whereupon the thermocouple was sealed off. While the vacuum was not at all good, the low heat conductivity of CCl_4 vapor occasioned a threefold increase in sensitivity—which was quite sufficient for the problem in hand. The sensitivity has not changed since the thermocouple was sealed off six months ago.

For dispersion measurements, the CCl_4 was procured from the Eastman Kodak Company, while the CS_2 was from Merck. Both of the highest attainable purity were subjected to further possible purification by two redistillations —the first and the last quarters being rejected. Finally, some freshly heated anhydrous copper sulphate was added and the liquids were allowed to stand a week. Measurements of the refractive

TABLE I.

λ	Refractive Indices of CS_2 at 20°C		λ	Refractive Indices of CS_2 at 20°C	
	Rubens	Pfund		Rubens	Pfund
0.5893μ	1.6275	1.6275	5.47μ		1.5112
.740	1.6090	1.6085	5.80		1.4812
.940	1.5993	1.5987	7.38		1.7247
1.32	1.5903	1.5904	7.62		1.6955
1.69	1.5862	1.5862	7.80		1.6849
2.41		1.5815	8.06		1.6711
3.21		1.5754	8.74		1.6486
3.92		1.5666	9.32		1.6381
4.32		1.5575	9.90		1.6316
4.67		1.5540	10.48		1.6277
4.84		1.5476	11.06		1.6244
5.14		1.5341			

TABLE II.

λ	Refractive Indices of CCl_4 at 20°C	λ	Refractive Indices of CCl_4 at 20°C	λ	Refractive Indices of CCl_4 at 20°C
0.5893μ	1.4607	5.90μ	1.4351	7.80μ	1.4254
.740	1.4541	6.11	1.4356	7.98	1.4248
.94	1.4517	6.22	1.4361	8.06	1.4223
1.32	1.4489	6.41	1.4360	8.45	1.4188
2.41	1.4466	6.60	1.4330	8.80	1.4219
3.92	1.4434	6.80	1.4315	9.02	1.4090
5.14	1.4387	7.20	1.4295	9.21	1.4036
5.47	1.4374	7.46	1.4274		

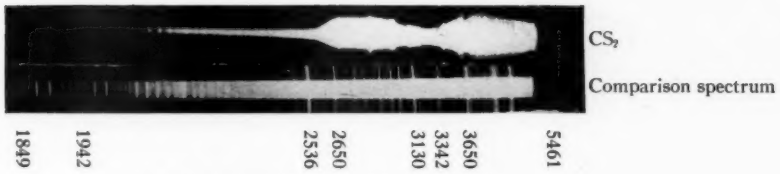

FIG. 3. Transmission of pure CS_2.

index μ carried out, both with the hollow glass-prism and an Abbe refractometer, yielded values identical with those accepted as correct[3]

$$CS_2 \quad \mu_D = 1.6275 \text{ at } 20.0°C,$$
$$CCl_4 \quad \mu_D = 1.4607 \text{ " " .}$$

The results on the dispersion of CS_2 are presented in Table I and Fig. 1 while those for CCl_4 are given in Table II and Fig. 2.

As is evident from Table I, the agreement of the present results with those of Rubens up to 2μ is quite satisfactory. No comparison data for CCl_4 appear to be available. In order to bring out more clearly the relation between dispersion and absorption, the transmission curves of both substances have been copied.[4] For CS_2 the weak absorption band near 4.6μ has only a slight effect upon the dispersion while the effect of the intense band near 6.7μ is very pronounced. The dotted portion of the dispersion curve (λ5896 $-$3904A) due to Flatow[5] is added to show how completely the infrared portion (7–11μ) is superimposed on the visible spectrum. In the case of CCl_4 the moderately strong absorption band at 6.45μ, while definitely producing anomalous dispersion, is secondary in importance to the intense band near 13μ.

While no attempt is here made to fit the results obtained to a dispersion formula, it did seem appropriate to determine more closely the positions of the absorption bands—particularly those in the ultraviolet. According to A. Pflueger's discussion of dispersion[6] the calculated position of the strong ultraviolet absorption band of CS_2 varies from 185 to 227 mμ. Since no direct determinations appear to have been made, a search was instituted for this band—the essential parts of the apparatus used being a quartz spectrograph with "oil-sensitized" plates, and a vacuum tube rich in CO lines near 2000A. At first it was found impossible to produce a CS_2 layer of sufficient thinness by forcing two plane quartz plates together. The experiment succeeded, however, by bringing a plano-convex quartz lens, whose curved surface had a radius of 12 cm into close contact with a plane fluorite plate. In air, the Newton black-spot had a diameter of about 1 mm. By filling then, the space between lens and plate with CS_2 and by bringing the vacuum tube, the black-spot and spectroscope into alignment, the spectrogram shown in Fig. 3 was obtained. The appearance of at least three CO bands between 1849 and 1942A makes it possible to determine the position of the center of absorption. The band was found to lie near 1965A. The weaker band is found, in accordance with previous workers, to lie near 3236A.

Because of the difficulty of getting the "black-spot" into alignment, the apparatus was modified, as shown in Fig. 4. Here A is a plano-cylindrical quartz lens (20 cm radius) whose curved surface has been cut away along the dotted lines. If now a plane quartz plate be pressed into contact with the remaining cylindrical strip, pressure being applied over the points 00, a black band about 1 mm wide and 1 cm long will have been produced. The aligning of this horizontal band with the vertical slit of the spectroscope is relatively easy. The results obtained were the same as those shown in Fig. 3.

While estimates of the thickness of layer within the Newton's dark-spot are difficult, it was found possible to form some concept by investigating the absorption of a dilute solution of CS_2 in ethyl alcohol. Repeated trials have

[3] Landolt Börnstein, Meyerhoffer, Phys.-Chem. Tabellen (1905), p. 671.

[4] W. W. Coblentz. *Inv. of Infrared Spectra* (Carnegie Institute, 1905).

[5] Flatow, Drudes Ann. **12**, 85 (1906).

[6] *Kayser's Handbuch der Spektroskopie*, Vol. IV (1908), p. 504.

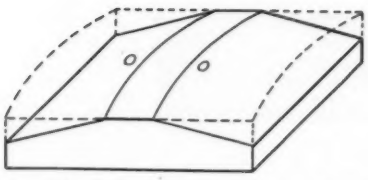

FIG. 4. Cylindrical quartz cell for transmission measurements of highly absorbing liquids.

shown that the positions and intensities of the absorption bands of CS_2 are not affected appreciably by ethyl alcohol. Photographs showing the same width of absorption as previously obtained for pure CS_2 were obtained at a concentration of 1:6000 and in a layer 0.04 mm thick. Such a layer contains pure CS_2 in a thickness of 7×10^{-6} mm.

It is therefore evident that, within the interval extending from 0.18μ to 11μ any calculation of the dispersion of CS_2 will have to take into consideration the following absorption bands:

λ		λ	
0.1965μ[7]	strong	6.61μ	strong
0.3236	weak	11.65[4]	weak
4.51	weak	13.4[4]	weak

[7] The 1965 band is known to be of electronic origin, hence its position ought not to be influenced greatly by the physical state of the material. This is substantiated by the work of W. C. Price (Washington Meeting Am. Phys. Soc., April 23, 1935; Phys. Rev. **47**, 788A (1935)) on CS_2 vapor. He finds a broad absorption band with its center near 1990A.

For liquid CCl_4 no determinations of the positions of the ultraviolet absorption bands have been made. Leifson[8] has found that CCl_4 vapor has two broad absorption bands, the first lying between 1840 and 1670A and the second extending from 1530 to shorter wave-lengths. Since here again the bands are of electronic origin, their positions ought to be essentially the same as in the liquid state. The positions of the principal centers of absorption for CCl_4, then, are:

λ	
0.1755μ	strong
6.45	weak
13.00[4]	strong

The attempt will shortly be made to follow the course of dispersion through the regions of strong absorption. Preliminary attempts with 2° prisms have been unsatisfactory. Not only is the accuracy unsatisfactorily low, but the opacity is still too great. A promising mode of procedure is the one[9] involving the production of interference fringes by partially silvered plates between which the liquid is confined. Since the thickness of layer may be reduced to less than 0.01 mm without sacrificing accuracy it will be possible to carry the measurements through the region of great absorption.

[8] S. W. Leifson, Astrophys. J. **63**, 87 (1926).

[9] A. H. Pfund, Zeits. f. Wiss. Phot. **12**, 346 (1913).

An Absorption Tube for the Investigation of Gases in the Photographic Infrared

RICHARD M. BADGER, LYMAN G. BONNER AND PAUL C. CROSS, *Gates Chemical Laboratory, California Institute of Technology*

(Received August 3, 1935)

An absorption cell of novel design is described, which combines the advantages of long path and relatively small volume.

IN the course of investigating the absorption of some polyatomic gases in the photographic infrared, in this laboratory, it was found that many interesting substances have a rather weak absorption which necessitates the presence of a very considerable amount of the material to be studied in the light path, to obtain absorption bands strong enough to photograph. This condition cannot in general be attained by using a high pressure of gas in a short absorption cell, since we have found in most cases no advantage in using pressures above one or two atmospheres due to the pressure broadening effect. For example, when the lines of an absorption band photographed at one atmosphere pressure are barely distinguishable on a spectrogram, because of weak absorption, an increase to three atmospheres in the same cell will in general result in little or no improvement as the increase in diffuseness of the lines counterbalances the greater absorption.

Consequently, in order to carry out a program of investigation which we had outlined, it appeared that an absorption cell of considerable length was necessary. An additional and conflicting requirement on the cell was that it have as small a volume as possible, since many of the substances to be investigated are difficult to obtain in large quantities.

It appeared to us that these two requirements were most easily satisfied by departing from the usual construction and using a tube of relatively small diameter with highly polished interior walls which would serve in place of the usual optical system to confine the light in the desired path. We accordingly constructed a cell seventy feet in length from stainless steel tubing of approximately 7/8 in. internal diameter, which had been provided by the manufacturer with a rather high polish on the interior wall. The tubing was obtained in five equal sections which were bolted together by means of flanges welded to the ends. A tongue or groove, respectively, in the opposing faces of a pair of flanges and a rubber ring gasket seated in the groove provide a satisfactory vacuum tight seal. The ends of the tube were closed with plates provided with plate glass windows seated in recesses and made tight either with sealing wax or rubber gaskets. Arrangements for evacuating the tube and for introducing various gases were provided.

Since it was proposed to study some substances which have relatively high boiling points, it was necessary to provide means of heating the tube. It was found that this was most conveniently done by passing a current through the tube itself. After the tube had been covered with ordinary steam pipe insulation it was found that a current of 86 amperes will maintain it a temperature of about 100°C. A potential of about 14 volts is required to pass this current.

It was somewhat difficult to predict what the optical efficiency of the absorption cell would be, but some estimates were made which were a guide in choosing the diameter of tubing to be used. The aperture of the spectrograph used in the investigations is such that of the light emerging from the absorption cell and entering the spectrograph slit only that making an angle of less than about 40′ with the cell axis will be caught by the grating. Because of this small angle the useful light in passing through the tube will have been reflected from the walls a maximum of ten times, and the greater part of it several times fewer. Furthermore, the reflection at these small angles is very efficient in the infrared, even with a relatively poorly reflecting material. The optical constants of the tube material were not available but assuming that they are not greatly different from those of ordinary high carbon

steel we estimated that our tube would be 75–80 percent as good as one made from a perfectly reflecting material.

This estimate was made on the assumption that the tube is a perfect cylinder, which it is not since it is slightly bowed in places and has minute ripples on the interior wall. However, we have recently made experiments in which a system of lenses was introduced into the cell which did not result in material improvement and showed that the arrangement worked nearly as well as could have been hoped.

Method of Illumination

The light source found most satisfactory is the ordinary double-filament automobile headlamp bulb. The two filaments are used simultaneously being connected in series, and are run at considerable overvoltage so that the life of the lamp is 24 hours or less. Not only is the cost of the lamps so low that a new one may be used for every exposure, if necessary, but they have proved as satisfactory as much more elaborate and expensive lamps. The light from the source is made nearly parallel as it enters the cell by means of the most powerful condensing lens practicable, which is fastened to the tube window. The position of the lamp is of course rather critical and micrometer screw adjustments are provided on its mounting.

For practical reasons the emergence end of the cell had to be about four feet from the spectrograph slit, necessitating the use of a lens between the two. We have had best results with a lens of about 70 cm focal length placed somewhat less than this distance from the slit.

The Spectrograph

The spectrograph used in conjunction with the absorption cell employs a 21-ft. concave grating with a 3×6-in. ruled surface, in an Eagle mounting. The grating was especially ruled for the purpose and in the photographic infrared throws most of the light in the first order on one side. With the arrangements as described and using Eastman infrared plates sensitized with ammonia the exposure times required are usually quite reasonable. Between the visible and λ10,300, where the sensitivity of the Eastman Q plates falls off rapidly, the exposure time ranges from fifteen minutes to four hours, provided the appropriate plates are used in each region.

Polarization-Interference Phenomena in Quartz Spectrographs

JOSEPH W. ELLIS AND JOSEPH KAPLAN, *University of California at Los Angeles*

(Received June 22, 1935)

SEVEN years ago in this laboratory, while photographing solar spectra with a Hilger E-1 quartz spectrograph, we observed numerous weak approximately equally spaced maxima and minima in addition to the Fraunhofer lines and bands. In connection with the discussion which is to follow it should be pointed out that the light became partially polarized at the surfaces of the mirrors used to direct the beam into the spectrograph.

In 1931 G. Bolla[1] presented some results on the Raman effect in water in which the usual broad Raman bands were striated in an unusual manner. He interpreted these striations as indications of a true rotational Raman spectrum. He later[2] corrected this interpretation, pointing out that the effect was one of interference arising in the totally reflecting prism in the spectrograph. The polarization required to produce this phenomenon existed in the scattered light beam. Rao[3] produced these striations with a Hilger E-1 instrument, completely polarizing the incident light with a Nicol prism. He showed that the spacings were equal to those in Bolla's Raman spectrum.

The effect was rediscovered in the physical optics laboratory here two years ago while students were photographing Haidinger fringes with the E-1 spectrograph. Light was plane polarized at a 45° azimuth and sent through two partially mirrored glass plates. The entrapped air film produced Haidinger fringe separations of the order of magnitude of those arising in the instrument, and a complicated pattern appeared on the plate exhibiting a kind of modulation effect. An effect similar to this has recently been displayed in a paper by Sundararajan.[4] In that instance, however, a single medium, namely, a thin section of a birefringent organic crystal produced both sets of fringes, those of the Haidinger type being the more closely spaced.

To gain a clearer concept of the origin of the fringes in the Hilger E-1 spectrograph we have produced a set of them between 6500 and 2500A, using a tungsten lamp and a carbon arc for sources. As Rao has pointed out, the fringes appear only when the light is at least partially polarized, and then only when the plane of polarization of the plane polarized portion of the beam makes an angle with the vertical other than 0° or 90°. Fig. 1 shows a portion of the fringes formed in the visible spectrum. The plate was carefully calibrated through the use of helium, neon and mercury lines and the wave number values of all of the measurable maxima and minima between 6500 and 3850A were determined. These wave number values have been plotted against an arbitrary set of numbers as shown in Fig. 2. The resulting graph is not a straight line. It becomes so, however, after each ordinate has been divided by an amount proportional to $(\mu_e-\mu_0)$, where μ_0 and μ_e are the ordinary and extraordinary indices of refraction for quartz. The justification for this procedure lies in the fact that it is a reflecting quartz prism acting as a thick wave plate which plays the dominant role in producing the fringes; and the equation for a wave plate may be written as

$$n=2(\mu_e-\mu_0)tv, \qquad (1)$$

where t is the plate thickness and n an integer (for certain wave numbers).

That an internally reflecting prism used as it is in the E-1 instrument can function as a wave plate is shown in Fig. 3. It is assumed that the optic axis lies in the prism faces. So long as the incidence is normal on the prism all rays, such as 1, 2, 3 travel equal paths through the prism. The light cone in the instrument is so small that the divergence among the rays is sufficient to introduce only a negligible disturbing effect.

A diagram of the complete optical system is shown in Fig. 4. Light from the source S passes through the Glan-Thompson polarizing prism P_1, the reflecting prism P_2, the crystalline quartz lens L, the dispersing prism P_3, and back to a

[1] G. Bolla, Nature **128**, 546 (1931).
[2] G. Bolla, Nature **129**, 60 (1932).
[3] I. R. Rao, Zeits. f. Physik **90**, 658 (1934).
[4] K. S. Sundararajan, Ind. J. Phys. **9**, 141 (1934).

FIG. 1. Polarization-interference fringes formed in the visible and near ultraviolet with a Hilger E-1 spectrograph.

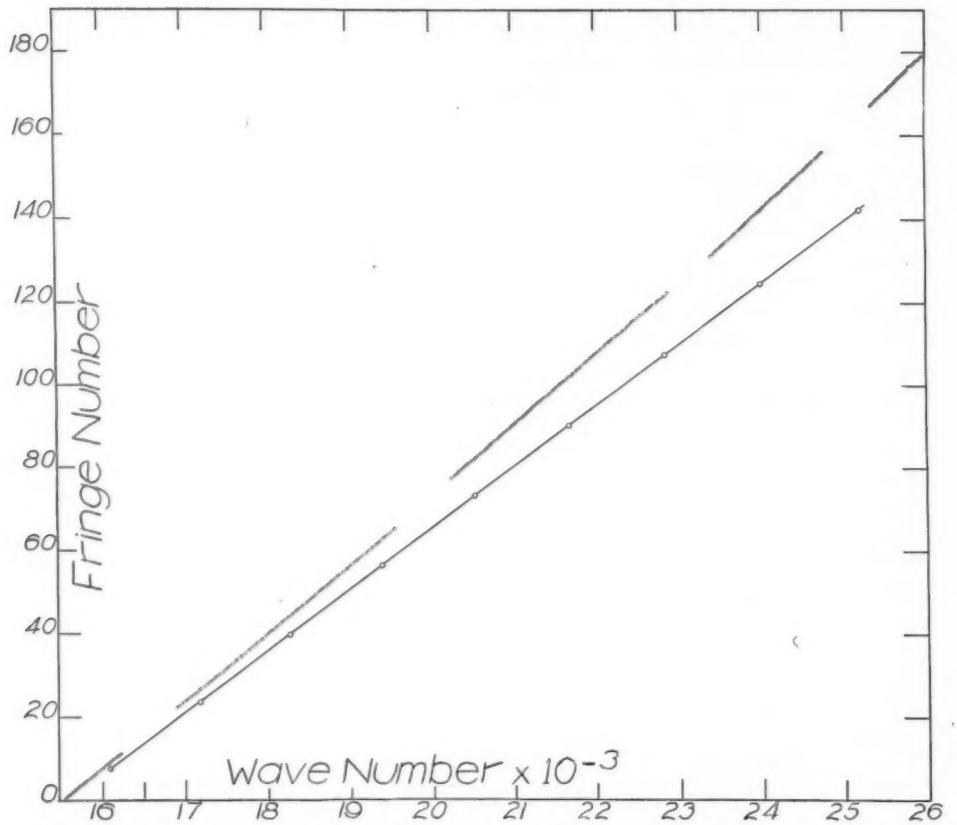

FIG. 2. Plot of wave number ν against fringe number n (arbitrarily assigned) of fringes from Fig. 1.

photographic plate I. To make the visibility of the fringes a maximum P_1 must be oriented so as to plane polarize the light at a 45° azimuth. The prism P_2 acts as a whole and as a half-wave plate for those wave numbers in Eq. (1) for which n is an even or an odd multiple of $\frac{1}{2}$, respectively. Waves of these two types will emerge from P_2 with their azimuths of vibration mutually at right angles. If the lens L were not optically active these two types of waves would each make a 45° angle with the plane of incidence of P_3, and, if Fresnel's reflection equations held at the face of P_3, would suffer equal reflection losses at this

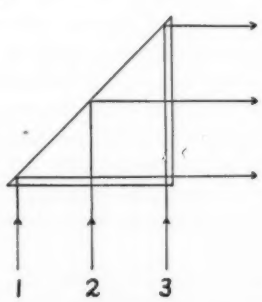

FIG. 3. A reflecting crystalline quartz prism may act as a wave plate.

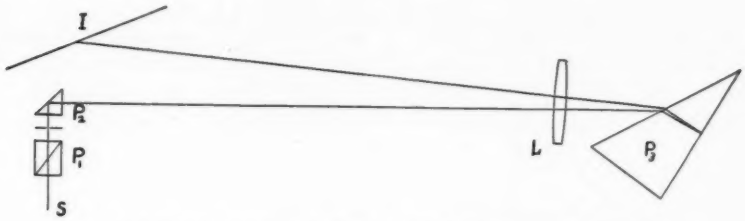

FIG. 4. The optical system of the Hilger E-1 quartz spectrograph.

face. No trace of wave-plate action in P_2 could then be detected in the spectrum formed at I. However, L is a crystalline quartz lens, 9 mm thick, with its optic axis coinciding with its geometrical axis. Thus all planes of vibration get rotated by this lens with the result that, in general, the vibrations of the two types of waves are inclined unequally to the plane of incidence of P_3. Thus one type of wave is transmitted with greater intensity than the other type and striations appear in the spectrum. There are positions of zero contrast, or zero visibility, in the spectrum, corresponding to those waves for which the rotation is such as to give equal inclinations with respect to the plane of incidence.

In passing through these regions of zero visibility while plotting Fig. 2, to maintain a continuous curve, it was necessary, of course, to assign to n even multiples of $\frac{1}{2}$ for the bright bands on one side and odd multiples on the other side. Although the fringe number assignments are arbitrary in Fig. 2, it can easily be shown from the 2 cm value of the thickness of P_2 that this prism acts as a 300th–800th wave plate for the region 6500–2500A.

A superficial examination of our visible and near ultraviolet interference spectrum led us to report to the American Physical Society[5] that the visibility minima occur at wave number intervals corresponding to changes of 90° in the rotation of the planes of vibration by the lens L. These intervals can be determined readily from the lens thickness (approximately 9 mm) and the rotatory dispersion of quartz. However, it was soon found, especially after the measurements were extended further into the ultraviolet, that after the first two the intervals deviate from 90°. They are alternately greater and less than 90°, varying in such a way that a long and a short interval together yield 180°. Fig. 5 shows the variations among these intervals. Near 2500A the short interval seems to have approached a zero value.

The cause for this variation in interval is not known to us, but it probably lies in the fact that Fresnel's equations, giving reflected and transmitted amplitudes in and perpendicular to the plane of incidence, do not hold at the surface of an optically active medium. That the phenomenon depends upon the angle of incidence is indicated by the fact that there is an irregularity in the diminution of the short interval in the neighborhood of 3300A. To go to wave-lengths shorter than this, adjustments have to be made in the instrument, and these include an alteration of the angle of incidence.

To get further information about these phenomena which were produced by the E-1 spectrograph, a Hilger E-2 spectrograph was employed. Since no reflecting prism is used in this instrument a quartz wave plate of about 2.3 mm thickness was introduced in the light beam in front of the slit. Not only did the usual striations appear in the spectrum but also the visibility minima were there with unequal intervals, thus proving that the phenomenon is not peculiar to the E-1 Littrow mounting.

Finally a Gaertner spectrometer with camera attachment was set up and equipped in turn with three different prisms. The light passed first through a polarizing prism, then through a 10-mm quartz wave plate and finally through a second 10-mm quartz plate cut with its optic axis perpendicular to its faces. This latter plate produced the necessary rotation of the planes of vibration. When a 60° flint glass prism was used

[5] Ellis and Kaplan, Phys. Rev. **47**, 255 (1935).

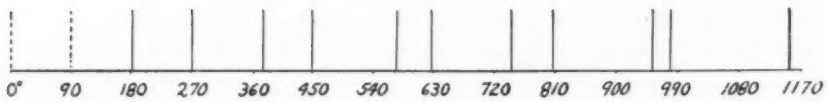

FIG. 5. Showing the departures of the centers of zero visibilities from the anticipated multiples of 90°.

for dispersion, clear-cut striations appeared with visibility minima at regular 90° intervals. Next a large 60° quartz prism cut with the optic axis parallel to the refracting edge and hence yielding two partially overlapping plane polarized spectra, was used. A Nicol prism was inserted in the beam before the glass collimator lens and oriented to remove completely one of the spectra. Visibility minima appeared at regular 90° intervals. Finally a Cornu prism was used but for some unknown reason it was impossible to secure clear-cut striations in the spectrum.

The regularity in the spacing of visibility minima yielded by the quartz prism whose optic axis lies in the surfaces, in contrast to the irregularity in spacing yielded by the E-1 and E-2 prisms whose axes do not lie in the surfaces, seems to indicate that the irregularities are produced somehow by further rotations in, or at the faces of, the latter prisms.

Maximum Visual Efficiency of Colored Materials

DAVID L. MACADAM, *Massachusetts Institute of Technology*

(Received August 2, 1935)

Tristimulus values have been computed for hypothetical spectrophotometric curves of the type found to give the maximum visual reflectance factor (or transmission factor) for specified chromaticities. These computations have been based on the I.C.I. 1931 data for the normal observer for colorimetry, and on the I.C.I. Illuminants "A" and "C." By plotting the results on the I.C.I. color mixture diagram, the loci of points characterized by equal maximum efficiencies have been established. Tables have been prepared showing the maximum visual efficiency as a function of excitation purity for twenty-four dominant wave-lengths.

ONE of the most compelling objectives of pigment and dye chemists has been to synthesize materials which could be used to produce colors of ever greater color purity without the sacrifice of brightness. The steady progress in this endeavor has led industrial users of colored materials to expect almost limitless improvements in these directions. This paper gives data which indicate that such improvements are possible in many directions, that not more than a few percent of the color possibilities have been realized to date. It also reveals that a physical limit has already been closely approached in some pigments and dyes, and that marked improvement is not to be expected in colors lying in these regions. These data will be most useful in indicating promising regions for research, and in preventing unreasonable demands for unattainable colors. In some cases, after specifying the dominant wave-length and purity desired in conjunction with a certain light source, designers of filters have requested visual transmission factors in excess of physically possible values. In other cases, opaque colored materials having visual reflection factors closely approaching the attainable limit for their chromaticity, have been criticized because these reflection factors were small compared to the unit reflection factor characteristic of a perfect white. Such criticism, and such unreasonable specifications are as unsound as criticism of the seemingly low efficiencies of well-designed heat engines operating between assigned temperatures that can be realized in practice. The purpose of a previous article[1] was to determine the characteristics of the most efficient colored materials. That work was analogous to the introduction of the concept of the perfect heat engine operating on the Carnot cycle as a standard of comparison against which engineers may make reasonable evaluations of the efficiencies of real heat engines. This paper presents data against which color technologists may make reasonable comparisons of the visual efficiencies of colored materials. It is analogous to the thermodynamic formula for the efficiency of a Carnot engine. However, the complicated behavior of this maximum attainable visual efficiency for various chromaticities makes it necessary to describe it by the use of tables and diagrams rather than by a simple formula such as occurs in heat engine theory.

The previous paper established the fact that the maximum attainable brightness corresponding to any desired chromaticity of a colored material under a given illuminant is secured if the material has a rather simple type of spectrophotometric curve. One condition for maximum brightness is that the reflection factor (or transmission factor) be either zero or unity at every wave-length of the visible spectrum. As a second condition, there must be no more than two transitions between zero and unity within the limits of the visible spectrum. The two classes of curves permitted are illustrated by the full lines in Figs. 1a and 1b. The wave-lengths of the transitions are determined by the quality of the illuminant and by the chromaticity desired. The brightness of a sample having such a spectrophotometric curve can be compared with the brightness of a perfect reflector under the same illumination by computation with the aid of standard visibility data and of data on the

[1] D. L. MacAdam, *Theory of the Maximum Visual Efficiency of Colored Materials*, J. O. S. A. **25**, 249–252 (1935).

FORM A. *Sample Calculation for Illuminant A.*
R = Visual efficiency = 0.60 (assigned).

	Column 1		Column 2	Column 3	
	$\sum_{\lambda_1}^{\lambda_2} yE = Y$				
	$= R \sum_{380}^{780} \bar{y}E = 6473.73$	$\lambda_2 = 583.87$ (interpolated from	$\sum_{380}^{\lambda_2} \bar{z}E = 3833.99$	$\sum_{380}^{\lambda_2} \bar{x}E = 3756.45$	
$\lambda_1 = 485.5$ (assigned)	$\sum_{380}^{\lambda_1} \bar{y}E = (+)158.00$	λ table)	$\sum_{380}^{\lambda_1} \bar{z}E = (-)3202.09$	$\sum_{380}^{\lambda_1} \bar{x}E = (-)560.22$	
	$\sum_{380}^{\lambda_2} \bar{y}E =$		$\sum_{\lambda_1}^{\lambda_2} \bar{z}E = Z = 631.90$	$\sum_{\lambda_1}^{\lambda_2} \bar{x}E = X = 3196.23$	$x = X/S = 0.3103$
	$\sum_{380}^{\lambda_1} \bar{y}E + \sum_{\lambda_1}^{\lambda_2} \bar{y}E = 6631.73$			$Y = 6473.73$	$y = Y/S = 0.6284$
				$Z = 631.90$	
				$S = X+Y+Z = 10301.86$	

FORM B. *Sample Calculation for Illuminant A.*
$R = 0.70$.

	$\sum_{\lambda_1}^{\lambda_2} \bar{y}E =$		$\sum_{380}^{780} \bar{z}E = 3837.57$	$\sum_{380}^{780} \bar{x}E = 11851.77$	
	$(1-R) \sum_{380}^{780} \bar{y}E = 3236.86$	$\lambda_2 = 551.43$	$\sum_{380}^{\lambda_2} \bar{z}E = (-)3823.93$	$\sum_{380}^{\lambda_2} \bar{x}E = (-)1259.05$	
$\lambda_1 = 485.5$	$\sum_{380}^{\lambda_1} \bar{y}E = (+)158.00$		$\sum_{\lambda_2}^{780} \bar{z}E = 13.64$	$\sum_{\lambda_2}^{780} \bar{x}E = 10592.72$	
	$\sum_{380}^{\lambda_2} \bar{y}E = 3394.86$		$\sum_{380}^{\lambda_1} \bar{z}E = (+)3202.09$	$\sum_{380}^{\lambda_1} \bar{x}E = (+) 560.22$	
	$Y = R \sum_{380}^{780} \bar{y}E = 7552.67$		$\sum_{380}^{\lambda_1} \bar{z}E + \sum_{\lambda_2}^{380} \bar{z}E = 3215.73 = Z$	$X = 11152.94$	$x = X/S = 0.5088$
				$Y = 7552.67$	$\bar{y} = Y/S = 0.3445$
				$Z = 3215.73$	
				$S = X+Y+Z = 21921.34$	

spectral distribution of energy in the illumination. This ratio of brightnesses has been called visual efficiency in the earlier communication. This term permits the simultaneous consideration of transparent and opaque reflecting materials and is used to represent interchangeably the concepts of visual transmission factors and of visual reflection factors.

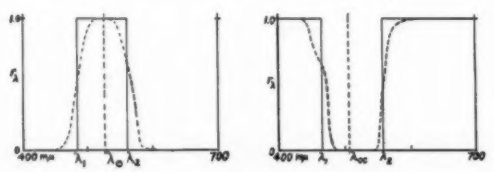

a b

FIG. 1a. Spectrophotometric curves for two green samples having dominant wave-length about 525 mμ and visual efficiency about 0.50. Box shaped curve, full line, has maximum attainable purity.

FIG. 1b. Spectrophotometric curves for two purple samples complementary to 505 mμ and having visual efficiency about 0.50.

Calculations intended for a general survey of the maximum visual efficiencies for all chromaticities might be planned in several ways since any two of five quantities may be considered as independent variables determining the values of the other three. For convenience of computation the visual efficiency to be attained and the shorter of the two transition wave-lengths have been assigned arbitrarily within limits imposed

TABLE I. *Points on loci of equal maximum efficiency.*

Results of computation for Illuminant A. Upper half of table is for curves similar to Fig. 1a. Lower half of table is for curves similar to Fig. 1b.

λ_1	λ_2	x	y	λ_2	x	y	λ_2	x	y	λ_2	x	y	λ_2	x	y
	$R=0.95$			$R=0.90$			$R=0.80$			$R=0.70$			$R=0.60$		
380.5	639.7	.4251	.4183	625.1	.4016	.4289	607.2	.3509	.4458	593.8	.3039	.4617	582.3	.2576	.4663
430.5	639.8	.4297	.4257	625.2	.4063	.4371	607.2	.3570	.4582	593.8	.3076	.4740	582.3	.2606	.4811
450.5	640.3	.4443	.4469	625.5	.4208	.4609	607.4	.3709	.4881	594.0	.3200	.5113	582.5	.2707	.5267
465.5	641.5	.4593	.4691	626.2	.4376	.4844	607.8	.3876	.5185	594.3	.3358	.5505	582.8	.2847	.5764
475.5	643.1	.4726	.4784	627.1	.4502	.4976	608.4	.4006	.5361	594.8	.3487	.5739	583.2	.2969	.6077
480.5							608.8	.4072	.5421	595.2	.3564	.5825	583.5	.3027	.6203
485.5	646.2	.4855	.4849	628.7	.4598	.5070	609.4	.4137	.5462	595.5	.3616	.5890	583.9	.3103	.6284
490.5							610.1	.4207	.5477	596.2	.3695	.5916	584.4	.3178	.6338
495.5				631.6	.4760	.5038	611.1	.4284	.5471	597.0	.3775	.5922	585.2	.3268	.6354
500.5				634.0	.4839	.5007	611.6	.4332	.5479	598.0	.3867	.5900	586.0	.3358	.6352
505.5							614.2	.4474	.5385	599.4	.3978	.5848	587.2	.3472	.6309
515.5							620.0	.4747	.5179	603.7	.4271	.5636	590.9	.3781	.6104
380.5	507.8	.5189	.4719	520.9	.5343	.4614	537.2	.5603	.4381	549.7	.5852	.4145	560.9	.6091	.3904
430.5	507.8	.5122	.4628	521.0	.5270	.4522	537.2	.5520	.4287	549.8	.5754	.4048	560.9	.5980	.3805
450.5	508.3	.4947	.4390	521.3	.5104	.4306	537.4	.5305	.4050	549.9	.5508	.3808	561.1	.5697	.3560
465.5	509.3	.4795	.4199	521.8	.4917	.4091	537.8	.5120	.3854	550.3	.5295	.3611	561.4	.5454	.3361
475.5	510.5	.4709	.4096	522.5	.4823	.3986	538.3	.5011	.3751	550.7	.5175	.3509	561.8	.5318	.3260
485.5	512.5	.4651	.4031	523.7	.4757	.3919	539.1	.4937	.3684	551.4	.5088	.3445	562.5	.5217	.3197
500.5	517.3	.4599	.3983	527.1	.4694	.3871	541.6	.4860	.3640	553.6	.4996	.3407	564.5	.5104	.3163
515.5				533.7	.4649	.3860	546.9	.4789	.3639	558.3	.4912	.3408	569.0	.4982	.3187
525.5										563.6	.4828	.3448	574.1	.4872	.3240
535.5													581.0	.4721	.3325
545.5										578.4	.4607	.3581	589.6	.4510	.3452
550.5				561.6	.4544	.3912	562.4	.4739	.3644	583.0	.4528	.3632	594.6	.4361	.3544
570.5	575.8	.4490	.4009	581.2	.4444	.3983	592.6	.4319	.3934	605.7	.4035	.3957			
590.5				603.2	.4282	.4096	619.4	.3904	.4221						

λ_1	λ_2	x	y	λ_2	x	y	λ_2	x	y	λ_2	x	y	λ_2	x	y
	$R=0.50$			$R=0.40$			$R=0.30$			$R=0.20$			$R=0.10$		
380.5	571.6	.2151	.4589	560.9	.1770	.4370	549.7	.1442	.3920	537.2	.1200	.3190	520.9	.1120	.1990
430.5	571.6	.2169	.4763	560.9	.1780	.4560	549.8	.1428	.4140	537.2	.1160	.3400	521.0	.1070	.2160
450.5	571.7	.2239	.5311	561.1	.1800	.5210	549.9	.1400	.4870	537.4	.1060	.4180	521.3	.0870	.2750
465.5	572.0	.2350	.5936	561.4	.1870	.5980	550.3	.1420	.5920	537.8	.0960	.5290	521.8	.0660	.3940
475.5	572.4	.2458	.6348	561.8	.1950	.6520	550.7	.1440	.6530	538.3	.0920	.6220	522.5	.0480	.5090
480.5	572.7	.2503	.6526												
485.5	573.1	.2588	.6639	562.5	.2070	.6940	551.4	.1530	.7100	539.1	.0940	.7070	523.7	.0390	.6340
490.5	573.6	.2663	.6724												
495.5	574.3	.2749	.6771												
500.5	575.1	.2850	.6780	564.5	.2340	.7180	553.6	.1800	.7510	541.6	.1220	.7790	527.1	.0550	.7750
505.5	576.3	.2972	.6750												
515.5	579.7	.3293	.6560	569.0	.2810	.7000	558.3	.2240	.7490	546.9	.1790	.7820	533.7	.1190	.8150
380.5	571.6	.6332	.3664	582.3	.6565	.3427	593.8	.6793	.3195	607.2	.7100	.3030	625.1	.7190	.2820
430.5	571.6	.6200	.3560	582.3	.6405	.3315	593.8	.6592	.3065	607.2	.6710	.2830	625.2	.6540	.2540
450.5	571.7	.5868	.3305	582.5	.6001	.3043	594.0	.6080	.2762	607.4	.6020	.2460	625.5	.5530	.2000
465.5	572.0	.5587	.3102	582.8	.5675	.2833	594.3	.5675	.2538	607.8	.5500	.2200	626.2	.4790	.1680
475.5	572.4	.5430	.3000	583.2	.5490	.2728	594.8	.5450	.2427	608.4	.5210	.2080	627.1	.4410	.1550
485.5	573.1	.5312	.2939	583.9	.5350	.2667	595.5	.5285	.2368	609.4	.4970	.2020	628.7	.4160	.1475
500.5	575.1	.5175	.2913	586.0	.5170	.2650	598.0	.5045	.2363	611.6	.4690	.2010	634.0	.3485	.1525
515.5	579.7	.5009	.2955	590.9	.4938	.2720	603.7	.4638	.2473	620.0	.4020	.2200			
525.5	585.0	.4841	.3033												
535.5	592.4	.4603	.3165												
545.5	602.1	.4243	.3370												
550.5	608.2	.3998	.3512												

by the nature of the problem. The longer transition wave-length has been calculated from these assigned quantities. The spectrophotometric curve is completely determined by the two transitions. Consequently the chromaticity can be computed from the knowledge of these transitions. The chromaticity may be described interchangeably in two manners, each involving two parameters. The first mode is the location by Cartesian coordinates of a point representing the sample in the color mixture diagram. The second mode is the location of this point by a species of polar coordinates. The polar coordinates are called dominant wave-length and purity. The angular coordinate, dominant wave-length, is measured by the wave-length of the spectral light whose chromaticity is represented by a point on the line through the sample point and the pole (the white point). If the points representing the spectral light and the sample are on opposite sides of the white point, the sample is said to be complementary to that dominant wave-length. This fact is indicated in this paper by a lower case "c" immediately following the wave-length of spectral light complementary to the color of the sample. The radial coordinate, purity, has been measured in

TABLE II. *Points on loci of equal maximum efficiency.*

Results of computation for Illuminant C. Upper half of table is for curves similar to Fig. 1a. Lower half of table is for curves similar to Fig. 1b.

λ_1	λ_2	x	y	λ_2	x	y	λ_2	x	y	λ_2	x	y	λ_2	x	y
	$R=0.95$			$R=0.90$			$R=0.80$			$R=0.70$			$R=0.60$		
380.5	627.3	.2857	.3185	611.7	.2631	.3192	592.1	.2236	.3120	578.4	.1932	.3005	567.1	.1694	.2797
430.5	627.7	.2943	.3395	612.0	.2697	.3410	592.3	.2282	.3382	578.5	.1953	.3263	567.2	.1698	.3065
450.5	630.2	.3226	.4055	613.4	.2956	.4111	593.2	.2465	.4183	579.3	.2064	.4136	567.8	.1732	.3995
465.5	635.0	.3608	.4679	616.0	.3302	.4827	594.8	.2743	.5056	580.4	.2261	.5163	568.8	.1847	.5156
475.5	642.1	.3907	.5025	619.2	.3590	.5232	596.6	.2991	.5591	581.8	.2495	.5835	570.0	.2011	.5982
480.5	648.7	.4055	.5126	621.6	.3742	.5364	598.0	.3136	.5784				570.8	.2117	.6316
485.5	662.7	.4209	.5180	624.8	.3896	.5438	599.6	.3284	.5913	584.0	.2733	.6282	571.8	.2238	.6567
490.5				629.3	.4020	.5493									
495.5				635.9	.4221	.5430	604.4	.3570	.5932	587.3	.3063	.6432	574.6	.2525	.6823
500.5				647.8	.4397	.5350	607.8	.3785	.5912	589.6	.3213	.6415	576.4	.2694	.6840
505.5										592.6	.3408	.6316			
515.5							628.1	.4493	.5433	601.2	.3876	.5999	585.1	.3344	.6502
525.5													594.9	.3908	.6016
535.5													611.0	.4605	.5364
380.5	488.5	.4300	.5195	504.8	.4555	.5235	523.1	.4901	.5038	535.8	.5187	.4780	546.7	.5470	.4514
430.5	489.0	.4070	.4720	505.1	.4295	.4741	523.2	.4562	.4505	535.9	.4795	.4243	546.8	.5004	.3963
450.5	491.3	.3630	.3855				524.0	.3966	.3584	536.6	.4107	.3319	547.3	.4217	.3042
465.5							525.4	.3631	.3103				548.3	.3803	.2593
475.5										538.9	.3566	.2675			
480.5	500.8	.3270	.3172	512.3	.3330	.3080									
485.5							529.0	.3391	.2815	540.7	.3460	.2578	551.1	.3500	.2330
500.5	512.2	.3160	.3069	520.7	.3230	.2975	533.9	.3304	.2754	545.0	.3356	.2525	555.2	.3376	.2284
515.5				530.0	.3180	.2958	541.6	.3229	.2756				562.1	.3238	.2294
525.5										558.5	.3185	.2544	568.9	.3132	.2322
550.5							571.2	.3035	.2802	583.2	.2875	.2651	598.5	.2593	.2497
570.5	576.2	.3053	.3096	582.4	.2980	.3030	597.4	.2747	.2926	620.6	.2290	.2868			
590.5				609.1	.2813	.3106	654.6	.2276	.3119						

λ_1	λ_2	x	y	λ_2	x	y	λ_2	x	y	λ_2	x	y	λ_2	x	y
	$R=0.50$			$R=0.40$			$R=0.30$			$R=0.20$			$R=0.10$		
380.5	556.8	.1510	.2520	546.7	.1383	.2180	535.8	.1302	.1764	523.1	.1289	.1268	504.8	.1363	.0692
430.5	556.9	.1497	.2785	546.8	.1350	.2425	535.9	.1255	.1980	523.2	.1230	.1438	505.1	.1308	.0792
450.5	557.5	.1462	.3736	547.3	.1246	.3363	536.6	.1092	.2845	524.0	.1027	.2152			
465.5	558.4	.1490	.5017	548.3	.1179	.4720	537.0	.0909	.4178	525.4	.0762	.3420	508.1	.0808	.2132
475.5	559.5	.1589	.5990				538.9	.0855	.5500	526.8	.0572	.4775			
480.5	560.3	.1677	.6411				539.0	.0836	.6110				512.0	.0371	.4135
485.5	561.2	.1782	.6750	551.1	.1343	.6800	540.7	.0911	.6700	529.0	.0500	.6250	513.7	.0251	.5007
490.5	562.4	.1913	.6980				541.3	.0975	.7140				515.6	.0181	.5893
495.5				553.6	.1596	.7377	542.7	.1100	.7487	532.0	.0637	.7410	517.8	.0181	.6718
500.5	565.4	.2222	.7185	555.2	.1766	.7470	545.0	.1294	.7700	533.9	.0787	.7747	520.7	.0276	.7416
505.5				557.1	.1952	.7500	546.3	.1462	.7806	536.1	.0992	.7975	523.2	.0434	.7890
510.5							548.7	.1698	.7793	538.7	.1239	.8055	526.4	.0687	.8178
515.5	572.8	.2867	.6936	562.1	.2437	.7305	551.4	.1957	.7696	541.6	.1518	.7983	530.0	.0996	.8252
525.5	580.5	.3412	.6493	568.9	.2964	.6903									
535.5	591.6	.4066	.5890	578.0	.3200	.6357									
380.5	556.8	.5759	.4231	567.1	.6065	.3925	578.4	.6390	.3613	592.1	.6717	.3273	611.7	.7040	.2946
430.5	556.9	.5207	.3655	567.2	.5395	.3320	578.5	.5530	.2950	592.3	.5542	.2513	612.0	.5126	.1913
450.5	557.5	.4304	.2737	567.8	.4347	.2410	579.3	.4300	.2040	593.2	.4077	.1603	613.4	.3424	.1028
465.5	558.4	.3844	.2309	568.8	.3833	.2000	580.4	.3733	.1658	594.8	.3463	.1263	616.0	.2813	.0771
475.5				570.0	.3607	.1851	581.8	.3485	.1528	596.6	.3195	.1150	619.2	.2518	.0693
480.5				570.8	.3527	.1807				598.0	.3075	.1122	621.6	.2378	.0674
485.5	561.3	.3489	.2071	571.8	.3453	.1777	584.0	.3300	.1462	599.6	.2968	.1104	624.8	.2230	.0663
495.5				574.6	.3325	.1752	587.3	.3140	.1443				635.9	.1868	.0664
500.5	565.4	.3347	.2026	576.4	.3260	.1750	589.6	.3045	.1447	607.8	.2586	.1104	647.8	.1628	.0676
515.5	572.5	.3175	.2046	585.1	.3003	.1783	601.2	.2643	.1503	628.1	.1918	.1182			
525.5	580.5	.3000	.2092	594.9	.2727	.1844									
535.5	591.7	.2746	.2162	611.0	.2276	.1955									
550.5	622.6	.2024	.2373												

several ways.[2] In this paper it will be measured in units of excitation purity which is simply the length of the line from the white point to the sample point divided by the length of the line through the sample point from the white point to the intersection with the locus bounding realizable chromaticities. This bounding locus consists of the spectral locus and the straight line joining the extremities of the spectral locus.

The computations were carried out according to the following forms.[3] Form A is for spectrophotometric curves of the type exhibited as a full line in Fig. 1a. Form B is for spectrophotometric curves of the type exhibited as a full line in Fig. 1b. In either case, arbitrary values of R and λ_1 were entered in the indicated spaces. The first two quantities in column 1 were secured from tables giving $\sum_{380\,m\mu}^{\lambda} E_\lambda \bar{y}_\lambda$ for I.C.I.

[2] D. B. Judd, *General Formula for Computation of Colorimetric Purity*, J. O. S. A. **21**, 729–747 (1931).

[3] For complete explanation of notation see J. O. S. A. **25**, 250 (1935).

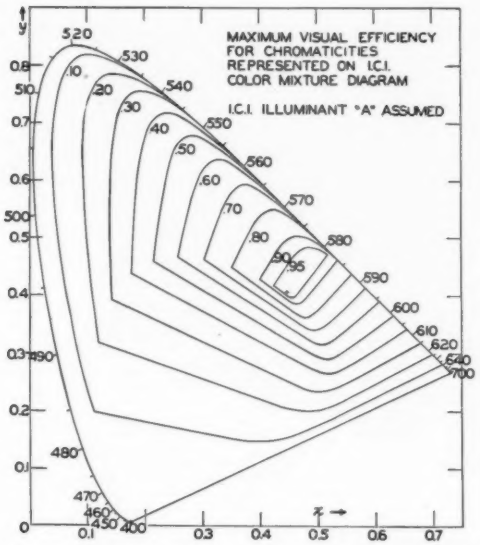

FIG. 2. Loci in I.C.I. color mixture diagram of points characterized by equal maximum visual efficiencies in Illuminant A. The values of maximum visual efficiency are indicated by numbers placed within the diagram near the corresponding locus. Numbers just outside the bounding locus indicate wave-lengths in millimicrons of spectral light represented by the associated points on that locus.

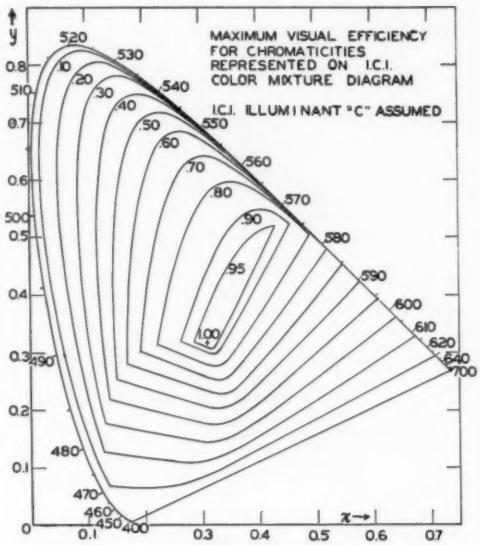

FIG. 3. Loci in I.C.I. color mixture diagram of points characterized by equal maximum visual efficiencies in Illuminant C. The values of maximum visual efficiency are indicated by numbers placed within the diagram near the corresponding locus. Numbers just outside the bounding locus indicate wave-lengths in millimicrons of spectral light represented by the associated points on that locus.

Illuminants A, B, or C as desired for λ at intervals of one millimicron from 380 mμ to 780 mμ. The third entry in this column was obtained by adding the first two entries. This total was then sought in the table for $\sum_{380}^{\lambda} E_\lambda \bar{y}_\lambda$ and λ_2 was interpolated and entered in the form. The entries in columns 2 and 3 were secured from similar tables for $\sum_{380}^{\lambda} E_\lambda \bar{z}_\lambda$ and $\sum_{380}^{\lambda} E_\lambda \bar{x}_\lambda$, respectively, and by carrying out the operations

TABLE III. *Maximum visual efficiency (%) of colored materials having indicated dominant wave-length and excitation purity for I.C.I. observer and Illuminant A.*

	Excitation Purity								
	0.10	0.20	0.30	0.40	0.50	0.60	0.70	0.80	0.90
λ =									
400mμ	61.0	41.0	29.5	20.5	14.5	10.0	7.0	4.5	2.0
470	63.0	43.0	31.5	23.0	17.0	12.5	9.0	5.0	3.0
480	66.0	46.0	34.5	27.0	21.0	16.0	13.0	10.0	6.0
490	73.5	55.0	43.5	36.5	31.0	27.5	24.0	21.0	12.0
495	80.0	64.5	54.0	47.0	41.5	37.0	33.0	22.0	10.0
500	86.0	75.0	67.0	61.5	54.5	43.5	32.5	22.0	11.0
505	90.0	81.0	71.5	61.5	50.5	40.0	29.5	20.0	12.0
510	90.0	80.0	70.0	60.5	50.0	40.0	31.0	22.0	13.0
520	89.5	80.5	72.0	63.5	54.5	46.0	37.0	27.5	17.5
540	93.0	86.5	80.0	74.0	68.0	62.0	55.0	47.5	37.5
550	95.0	90.0	85.0	80.5	76.0	71.5	66.5	61.0	49.5
560	96.5	93.5	89.5	86.5	83.0	80.5	77.5	73.5	65.5
570	98.5	97.0	95.5	94.0	92.0	90.0	87.5	84.5	78.5
575	99.5	99.0	89.5	98.0	97.0	95.5	94.0	91.5	87.5
580	100.0	100.0	100.0	100.0	99.5	99.5	99.0	98.5	96.5
585	98.5	97.0	95.5	94.0	92.5	91.0	90.0	88.5	86.5
590	97.5	94.5	92.0	89.5	86.5	84.0	82.0	79.5	77.0
600	95.5	90.5	85.0	80.0	75.5	71.0	66.0	61.0	56.5
700	91.0	81.0	71.0	61.0	51.0	41.5	33.0	23.5	12.5
510c	91.5	81.5	72.5	64.0	54.0	44.5	35.5	25.5	15.0
550c	89.0	78.0	68.0	58.5	51.0	44.0	35.5	25.5	14.5
570c	80.5	64.0	51.5	42.5	35.5	29.5	23.5	17.0	12.0
575c	72.0	53.0	41.0	33.0	25.5	20.0	15.5	11.5	6.5
579c = 400	61.0	41.0	29.5	20.5	14.5	10.0	7.0	4.5	2.0

TABLE IV. *Maximum visual efficiency (%) of colored materials having indicated dominant wave-length and excitation purity for I.C.I. observer and Illuminant C.*

	Excitation Purity								
	0.10	0.20	0.30	0.40	0.50	0.60	0.70	0.80	0.90
λ =									
400mμ	81.0	65.5	53.0	41.0	32.0	24.0	17.0	11.0	5.5
470	82.5	68.5	57.5	47.0	37.5	30.5	24.0	18.0	12.5
480	86.0	74.0	64.5	56.0	48.5	41.0	34.5	29.5	16.0
490	92.5	85.5	80.0	73.0	62.0	50.0	38.0	26.0	14.5
495	93.0	86.0	79.0	69.0	58.0	46.0	35.5	25.0	14.5
500	92.0	84.0	75.5	66.5	55.5	44.5	34.0	24.5	15.0
505	91.0	82.5	73.0	63.5	53.5	43.0	33.5	24.0	15.5
510	91.0	83.0	74.0	64.0	54.0	44.5	35.5	26.5	17.5
520	92.0	84.0	76.0	68.0	59.5	51.5	43.0	34.0	23.0
530	93.0	87.0	81.0	74.5	68.5	62.5	56.0	48.5	37.5
540	95.0	90.5	86.0	82.0	77.5	73.0	68.0	62.5	54.0
550	97.0	94.0	91.0	88.0	85.5	82.0	78.5	74.0	64.0
560	98.5	97.0	95.5	94.0	92.5	91.0	88.5	85.5	80.5
570	99.5	99.0	98.5	98.0	97.5	97.0	96.0	95.0	88.5
580	96.5	93.5	90.5	87.5	84.5	81.5	78.5	76.0	73.5
590	93.5	87.0	81.0	75.0	69.5	64.5	60.5	57.0	53.5
600	91.0	81.5	72.5	64.5	57.5	51.5	46.0	41.5	38.0
620	87.0	74.0	62.0	52.5	43.5	36.0	29.5	24.0	19.0
700	84.0	70.0	56.5	44.5	34.5	26.5	20.5	14.0	7.0
495c	86.5	73.0	60.5	49.5	39.5	30.5	22.5	15.0	7.5
500c	89.0	77.5	66.5	55.5	45.0	35.0	26.0	16.5	7.0
510c	90.5	80.0	70.0	60.0	50.0	40.0	30.0	20.0	10.0
550c	88.0	76.5	66.0	55.5	47.0	38.5	30.5	22.5	13.0
560c	84.0	70.5	59.5	49.0	39.0	31.0	24.0	17.5	10.0
567c = 400	81.0	65.5	53.0	41.0	32.0	24.0	17.0	11.0	5.5

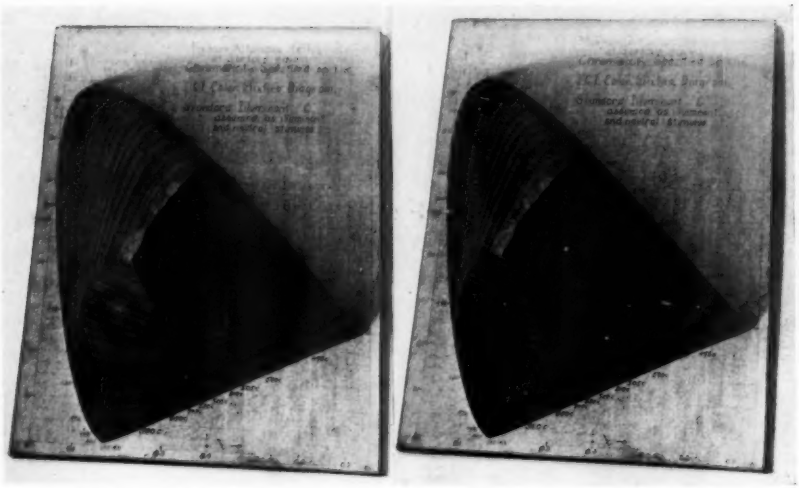

FIG. 4. Stereoscopic photograph of surface bounding all attainable colors in Illuminant C. Base of this solid is I.C.I. color mixture diagram. The vertical axis is visual efficiency. This surface is fully defined by Fig. 3, which may be regarded as a contour map.

indicated by the algebra and the symbols in parentheses. The values of x and y were then determined as indicated.

Table I shows the results of about two hundred such computations for Illuminant A. Table II shows similar results for Illuminant C. These tables are published with the above computation forms for the guidance of workers who may desire to investigate more fully small regions of chromaticity having special interest and who require a denser distribution of points in such regions. The tables of the running sums used as the basis for these computations are easily prepared from tables to be published soon.

Figs. 2 and 3 exhibit these results as loci in the color mixture diagram of points having constant maximum visual efficiencies. For some purposes it is convenient to represent colors by points in a three-dimensional space consisting of a visual efficiency coordinate axis perpendicular to the usual chromaticity axes of the color mixture diagram. Figs. 2 and 3 may be regarded as contour maps of surfaces enclosing points representing in this three-dimensional space all attainable colors of materials. Fig. 4 is a stereoscopic photograph of this surface for Illuminant C.

Tables III and IV give maximum attainable

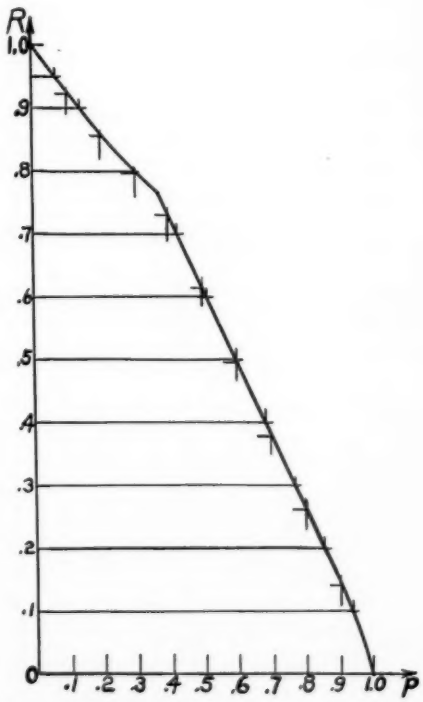

FIG. 5. Maximum visual efficiency plotted against excitation purity for one representative dominant wavelength, 490 mμ. This plot was prepared graphically from Fig. 3, i.e., for Illuminant C.

visual efficiency as a function of the chromaticity variables, namely, dominant wave-length and excitation purity for Illuminants A and C. These values were secured by graphical construction from Figs. 2 and 3. The dominant wave-length loci were drawn on these figures. The lengths of the segments of each of these loci from the white point to the intersections with the successive efficiency loci were plotted against the corresponding value of the visual efficiency. Smooth curves were fitted appropriately through these observed points, discontinuous slopes being allowed corresponding to the two ridges in the three-dimensional surface shown above. The maximum visual efficiency corresponding to desired values of excitation purity was then found by locating the point on these curves at the corresponding fraction of the distance from the white point to the spectral locus. Fig. 5 illustrates this method for Illuminant C and for dominant wave-length 490 mμ.

Examination of the sources of error in these calculations will show that the values given in Tables I and II should be accurate to ± 0.001. Figs. 2 and 3 have been drawn carefully and it is unlikely that any points on the loci are in error by greater than ± 0.005 in either of the coordinates. The double chance for errors in graphical construction to enter in the preparation of Tables III and IV makes it seem unwise to rely on these values of maximum visual efficiency to better than ± 0.5 percent.

The author wishes to express his sincere appreciation of the interest and assistance of Professor A. C. Hardy during the preparation of this material.

The Luminescence of Frozen Solutions of Certain Dyes

FRANCES G. WICK AND CHARLOTTE G. THROOP, *Vassar College and Cornell University*

(Received August 19, 1935)

MANY organic dyes which show no luminescence in the solid state are luminescent in solution, the intensity varying with the nature of the solvent, the concentration, and the temperature. The work described in this paper was undertaken to study the luminescence of a number of dyes in different solvents from room temperature down to that of liquid air.

From a large collection of DuPont dyes kindly placed at our disposal by Dr. D. R. Morey, many of which show fluorescence in solution when excited by violet and ultraviolet light at room temperature, a number were chosen for preliminary observation under excitation of a carbon arc through a Corning ultraviolet filter. The dyes were dissolved in water, acetone, ethyl alcohol and glycerine each dye in those solvents in which it was easily soluble. As the temperature of the solution was lowered striking and often abrupt changes in the intensity and in the color of the luminescence were observed. Many of the frozen solutions are phosphorescent.

The alcohol, acetone and glycerine solutions continue to show luminescence at all temperatures down to that of liquid air with variations in color and brightness. A few of the water solutions behaved in a similar way showing continued luminescence down to the lowest temperature observed. Others ceased to luminesce at the freezing point and showed luminescence of a different color at a much lower temperature. Still others showed no luminescence below the freezing point of water.

Naphtha Sultam, rhodamin B—extra and uranine each representing, respectively, one of the types of behavior in water solution were selected for special study. Intensity measurements of various concentrations of the dyes in solution were made and, upon the basis of these, a 1/2500 gram molecular solution was selected for all observations.

The fluorescence spectra of the solutions studied, observed through a direct vision spectroscope, show broad bands which narrow and resolve to different degrees in the various solvents as the temperature is lowered. In some cases certain bands become dimmer and disappear and others brighten or new bands appear. Rough observations of the region of the spectrum effective in exciting fluorescence were made by placing the solutions in small quartz tubes and exposing them to radiations from a tungsten spark dispersed by a system of quartz lenses and prisms. There are, in general, two regions of excitation, one in the ultraviolet and one in the visible, the color of the luminescence excited by these bands being different, in many cases. The regions of excitation appeared to be the same for a given dye in the various solvents used. The duration and brightness of phosphorescence of the frozen solutions was found to vary with the solvent.

METHOD OF OBSERVATION

An arrangement of apparatus similar to that used by Nichols and Howes,[1] as shown in Fig. 1, was used to make exact comparisons of intensities of luminescence under different conditions of concentration and temperature. A test tube *T*, containing a few cc of the solution under observation was mounted in a cylindrical copper block, *B*, in the side of which a channel was cut for the admission of the exciting light and the observation of the fluorescence at right angles to it. To the bottom of this block was soldered a copper tube, *D*. This copper mounting was supported by rods *A* so that it could be lowered to different depths in liquid air contained in a tall, unsilvered Dewar flask, *F*. Variations in temperature thus obtained were measured by a thermojunction *J* placed in the solution. A lamp, *L*, mounted so that it could be placed in the copper tube, *D*, was used to raise the temperature of the solution above that of the room before starting a run, and to aid in bringing the block back to room temperature after a run had been completed.

Luminescence was excited by light from a Westinghouse "black bulb" lamp, the light from

[1] Howes, Phys. Rev. **6**, 193 (1915).

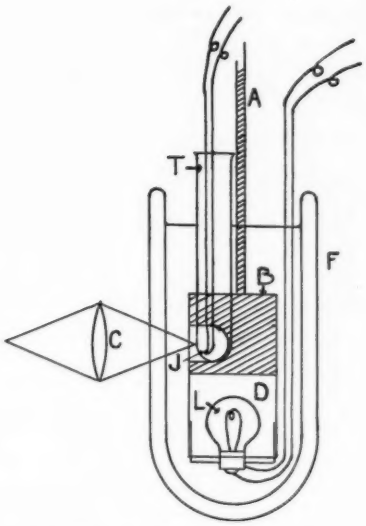

FIG. 1. Apparatus for making intensity measurements of fluorescent dye solutions at low temperatures.

which was focused on the specimen by a glass condensing lens, *C*. This source of illumination was found to be of constant intensity. Brightness measurements were made, at right angles to the exciting light, by means of a Leeds and Northrop optical pyrometer with a color filter in the eyepiece transmitting only a narrow spectral band matching, as nearly as possible, the luminescence band in the solution under observation. For specimens showing two prominent luminescence bands two sets of observations were made using different filters. The brightness of luminescence was determined by adjusting the current through the pyrometer lamp until the intensity of the filament matched that of the specimen. By using the calibration of the lamp the effective temperature in degrees F was determined and from this, with the data given by Forsythe,[2] the brightness of the specimen in candlepower per square cm was computed.

URANINE

In water solution the fluorescence of uranine is very bright and has a green color. In alcohol, acetone and glycerine the color is yellower than in water solution becoming greener at lower temperatures. The spectrum of the water solution shows a broad band the approximate limits of which are wave-lengths 5500–6500A. The band in the alcohol and glycerine solutions extends from about 5000 to 6000A. The band in the glycerine solution resolves, at the temperature of liquid air, into two bands the approximate limits of which are 5300 to 5500A and 5700 to 5850A. The region most effective in excitation is 2200 to 4500A with a maximum at about 2600A. Another exciting region somewhat less effective extends from 4500 to 5000A. The frozen water solution shows no phosphorescence, the alcohol solution shows, at liquid air temperature, yellowish green phosphorescence of long duration, and the glycerine solution has a yellow phosphorescence of shorter duration at a somewhat higher temperature.

The intensity of fluorescence at room temperature was measured in widely different concentrations with a blue-green Wratten No. 44 filter in the eyepiece of the pyrometer transmitting approximately wave-lengths 4300 to 5550A. Fig. 2 shows the results of these observations, curve 1 for the water solutions, curve 2 for the alcohol solutions. In each of these a sharp maximum is seen, the optimum concentration being greater for water than for alcohol.

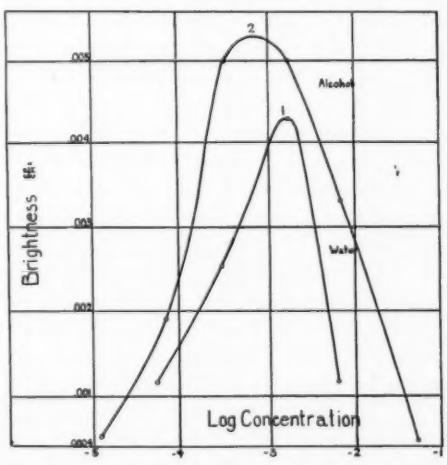

FIG. 2. Brightness of fluorescence of different concentrations of uranine solutions. Curve 1, water solution; curve 2, alcohol solution.

[2] Forsythe, J. O. S. A. **16**, 307 (1928).

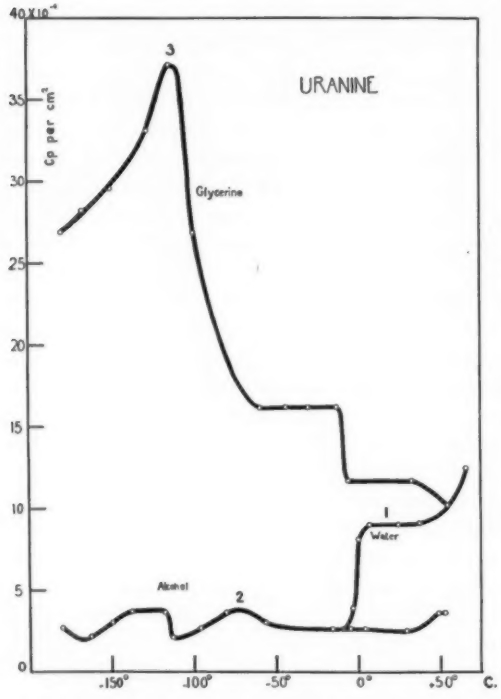

FIG. 3. The effect of decreasing temperature on the brightness of uranine solutions. Curve 1, water solution; curve 2, alcohol solution; curve 3, glycerine solution.

The variation in intensity of luminescence of a 1/2500 gram-molecular solution of uranine in different solvents is shown in Fig. 3. In water solution the fluorescence is suddenly quenched at the freezing point as shown in curve 1. In alcohol solution, shown in curve 2, there are two points of inflection, one at the freezing point of alcohol, −114°C, the other at about −148°C. In glycerine solution, curve 3, there is a point of inflection at the freezing point of water, one at −83°C and one at −100°C.

These sudden inflections indicate changes in physical condition of the solvents. Observations of Gibson and Giauque[3, 4] upon the changes in specific heat of alcohol and of glycerine upon lowering of temperature show that, at the points of inflection shown in Fig. 3 there are sudden changes in specific heat accompanied by changes in physical condition.[3] Pure ethyl alcohol cooled

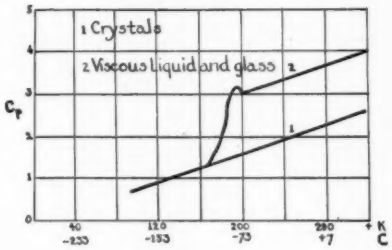

FIG. 4. Heat capacities per mean gram atom for supercooled and crystalline glycerol plotted against temperature.

slowly forms crystals at the freezing point, −114°C; cooled rapidly the alcohol undercools to a viscous liquid with higher specific heat than the crystals. At −148°C it reaches a jelly-like consistency and, on further cooling, undergoes a noticeable contraction and solidifies to a hard, transparent glass.

The points of inflection of curve 3 coincide with temperatures at which abrupt changes in the physical condition of glycerine occur upon cooling. The melting point of pure glycerine is 18°C. Below this point it may exist as crystals with low specific heat or may be undercooled to a viscous liquid with low specific heat as shown in Fig. 4, a curve taken from the work of Gibson and Giauque.[4] At −83°C the viscous liquid changes suddenly and becomes a hard, transparent glass. At this point of transition there is a sudden change in brightness of all fluorescent solutions observed in which glycerine is the solvent.

RHODAMIN B-EXTRA

Rhodamin B-extra has an orange-yellow fluorescence which is strong in all solvents but of greater intensity in alcohol and in glycerine than in water and in acetone. In water solution the spectrum is continuous between the approximate limits 5600 and 6500A with the greatest intensity in the yellow. At the freezing point this band disappears and the solution shows no luminescence until a temperature of about −50°C is reached when a sharp red band appears with limits about 6100 to 6500A. This

[3] Gibson and Giauque, J. Am. Chem. Soc. **42**, 1542 (1920).

[4] Gibson and Giauque, J. Am. Chem. Soc. **45**, 93 (1923).

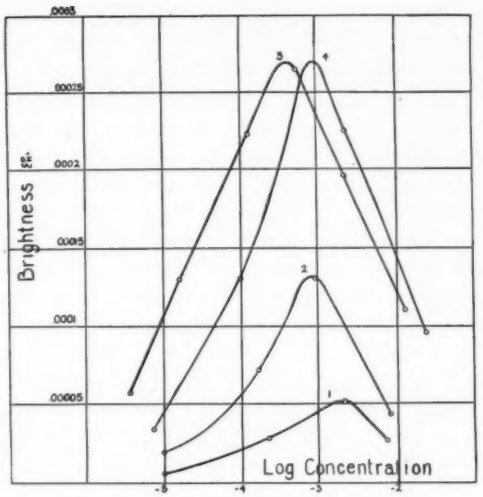

FIG. 5. Brightness of fluorescence of different concentrations of rhodamin B-extra solutions. Curve 1, water solution using red filter; curve 2, water solution using yellow-green filter; curve 3, alcohol solution using yellow-green filter; curve 4, alcohol solution using red filter.

band becomes very bright as the temperature is lowered. The changes which take place in a rhodamin water solution upon lowering of temperature may be simultaneously observed by lowering a test tube containing the solution into an unsilvered Dewar flask containing liquid air, keeping the top of the solution above the level of the air so that it remains liquid with the orange-yellow fluorescence while the bottom quickly reaches the temperature of liquid air and shows red luminescence. Between the two ice is formed which is not cold enough to show any luminescence. The carbon arc through a Corning ultraviolet filter was used for these observations. In alcohol solution at room temperature there is a broad band which extends from about 5700 to 6600A. At low temperatures the blue end disappears and the band becomes sharper having limits about 5800 to 6000A. A red band appears between 6300 and 6500A. In acetone the broad band which at room temperature extends from 5600 to 6600A changes to a sharp band between 5900 and 6000A at liquid air temperature. No phosphorescence is shown by the water frozen solution. The frozen alcohol solution shows phosphorescence of longest duration. The acetone solution shows phosphorescence the color of which is green when the physical condition is glassy and yellow or orange when the condition is crystalline.

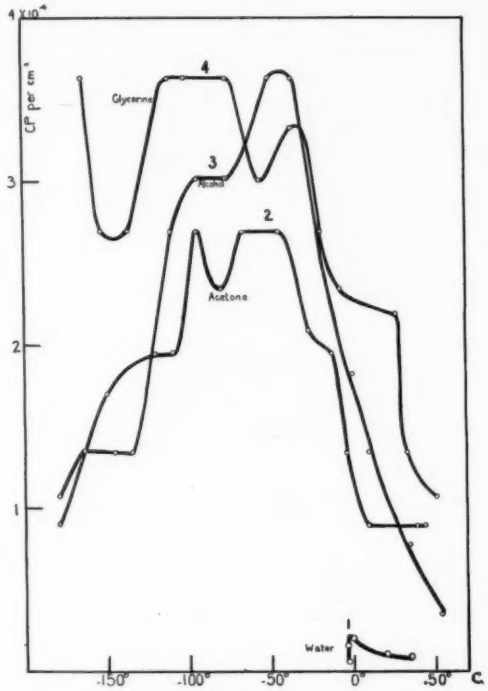

FIG. 6. The effect of decreasing temperature on the brightness of rhodamin B-extra solutions using yellow-green color filter. Curve 1, water solution; curve 2, acetone solution; curve 3, alcohol solution; curve 4, glycerine solution.

The intensity of fluorescence at room temperature was measured in widely different concentrations in alcohol and in water solutions through two different filters—a red filter Wratten No. 25 transmitting wave-lengths 5750 to 7000A and a green-yellow filter Wratten No. 66 plus Aero No. 3 transmitting wave-lengths 4600 to 6500A. Fig. 5 shows the results of these observations. In both solvents the optima through the red filter, curves 1 and 4 are of higher concentration than those through the green-yellow filter, curves 2 and 3. Through both filters the optimum concentration for the water solution is greater than for the alcohol solution. This is also the case for uranine as previously observed and shown in Fig. 2.

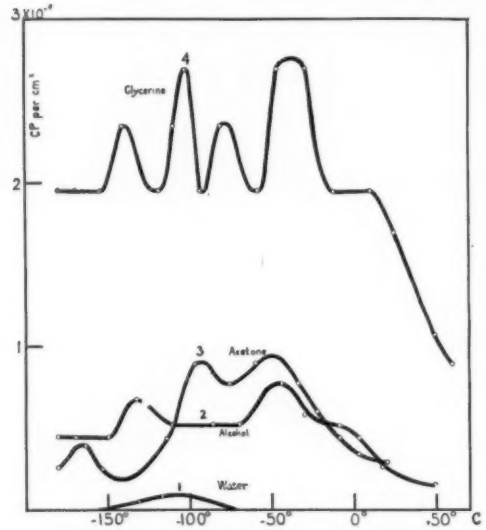

FIG. 7. The effect of decreasing temperature on the brightness of rhodamin B-extra solutions using red color filter. Curve 1, water solution; curve 2, alcohol solution; curve 3, acetone solution; curve 4, glycerine solution.

The effect of temperature upon a 1/2500 g molecular solution of rhodamin B-extra in different solvents using the yellow-green filter in the eyepiece is shown in Fig. 6. Curve 1 shows that the luminescence of the water solution which is very weak compared with the other solutions drops suddenly to zero at the freezing point. The acetone solution, curve 2, increases in intensity at the freezing point of water and has a sudden drop at the freezing point of acetone, −94.3°C. The alcohol solution, curve 3, shows marked increase at the freezing point of water and a marked decrease at the freezing point of alcohol, −114°C. Below −148°C, the temperature at which glass is formed, the intensity decreases. The glycerine solution, curve 4 shows an increase at 50°C, the point at which pure glycerine solidifies. There is an increase at the freezing point of water and another increase at −83°C where the viscous liquid changes to glass. Other points of inflection may indicate intermediate states of aggregation.

Fig. 7 shows intensities at various temperatures with a red filter transmitting 5850–7500A. The water solution, curve 1 shows the appearance of the red band only at low temperatures reaching a maximum at about −110°C. The alcohol solution, curve 2 shows no change at the freezing point of water; at −114°C, the freezing point of alcohol, there is an increase in intensity; at −148°C the temperature below which the solution forms glass the intensity is less. The acetone solution, curve 3 shows two maxima below the freezing point of water one of which is at the freezing point of acetone, −94°C—these same two maxima are observed through the yellow filter, Fig. 6, curve 2. The glycerine solution, curve 4, shows irregularities. An increase takes place at 18°C, the temperature at which pure glycerine solidifies. Evidently a change in molecular state takes place at this same temperature in the glycerine containing water.

NAPHTHA SULTAM

This dye is soluble in all four of the solvents used showing fluorescence which ranges in color from green to blue in different solvents and at different temperatures. The water solution at room temperature has a green color with a spectrum showing a continuous band from about 4250 to 6500A the most intense part of the spectrum being between 5000 and 5500A. A change in color from green to blue takes place suddenly as the temperature is lowered which shows a fluorescence band having the same spectral limits but a different distribution of intensity the maximum being between 4500 and 4750A. The region of excitation is between 2100 and 4500 with maxima at 2800A, and between 3800 and 4000A. Phosphorescence of longest duration and greatest brightness was observed in the frozen solution of acetone, glycerine coming next and alcohol last. The water solution showed no phosphorescence.

Two sets of temperature-intensity observations for the water, alcohol and glycerine solutions of concentration 1/2500 were made one through a green filter, Wratten No. 44 transmitting wave-lengths 4300 to 5550A, the other through a blue filter, Wratten No. 46 transmitting wave-lengths 4400 to 5250A. The curves showing the results through the green filter are shown in Fig. 8.

Curve 1 for the water solution shows that the luminescence is not quenched at the freez-

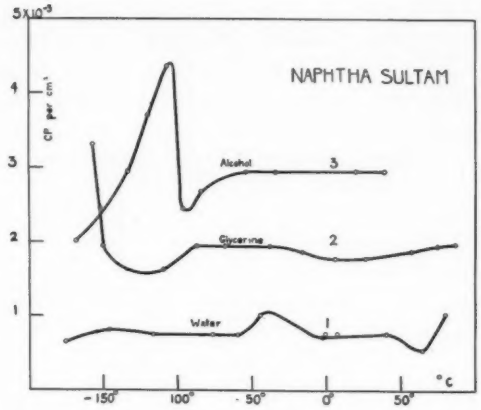

FIG. 8. The effect of decreasing temperature on the brightness of Naphtha Sultam solutions using green filter. Curve 1, water solution; curve 2, glycerine solution; curve 3, alcohol solution.

ing point. The intensity begins to increase at this point and continues to increase to about −40°C then decreases to about −60°C below which temperature the intensity remains practically constant. Curve 2 for the glycerine solution shows little change in brightness until the solution reaches the temperature −83°C where the solution changes from viscous liquid to glass at which point there is a decrease in intensity with a minimum at −125°C. At −150°C there is a sudden increase in brightness. Curve 3 for the alcohol solution shows a minimum just before the temperature of solidification of alcohol, −114°C, then, at this temperature an abrupt increase in intensity followed by a sudden decrease. The curves for alcohol and glycerine 2 and 3, Fig. 8 show no break at the freezing point of the water solution since the luminescence of the water solution is not extinguished or sharply changed at this point.

Fig. 9 shows the temperature-intensity curves through a blue filter Wratten No. 46, transmitting wave-lengths 4400 to 5250A. The brightness of luminescence through this filter was much greater than that through the green filter. Curve 1 for water shows an increase in intensity up to the freezing point, then, at this point, a sudden drop with a minimum at about −25°C. From this point there is a rapid increase to about −75°C at which point the brightness

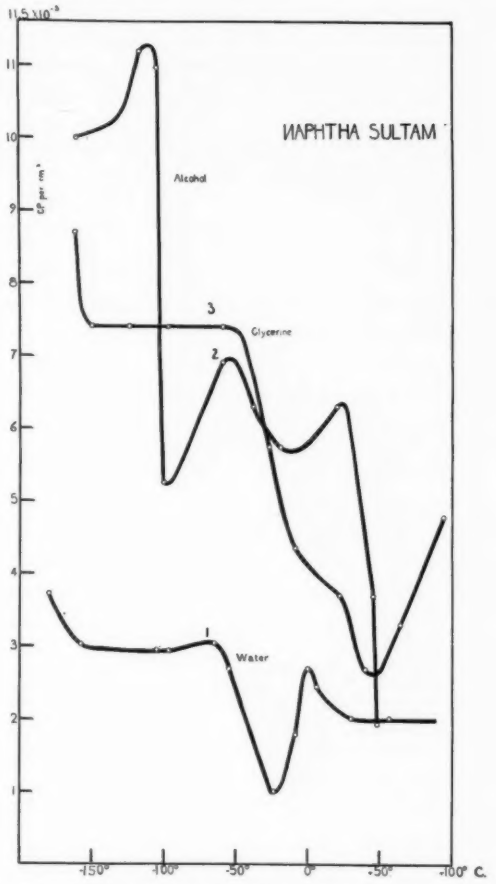

FIG. 9. The effect of decreasing temperature on the brightness of Naphtha Sultam solutions using a blue filter. Curve 1, water solution; curve 2, alcohol solution; curve 3, glycerine solution.

becomes practically constant at a higher intensity than that of lower temperatures. Curve 2 for alcohol shows a rapid increase as the temperature is lowered from plus 50 to zero, then a slight decrease with a minimum at 0 degrees. This is followed by a maximum, then comes a minimum just before the freezing point of alcohol is reached. At this point there is a sharp maximum followed by decreasing intensity. Curve 3 for glycerine shows a point of inflection at the melting point of glycerine, 18°C, then an abrupt increase at the temperature giving a minimum for water, probably due to water in the glycerine.

In the work described in this paper no attempt

was made to obtain solvents free from water. The presence of water in the various solutions is indicated by changes in the intensity of luminescence at the freezing point of water in the alcohol, acetone and glycerine solutions of a dye which shows marked changes at the freezing point in water solution.

Summary

The luminescence of organic dyes in solution shows marked changes in intensity when the solutions are cooled to the temperature of liquid air. These changes are observed to take place at temperatures at which the physical condition of the solvent changes such as in freezing, in change to a viscous liquid and in change from a viscous liquid to a hard, transparent glass. These changes in luminescence are of such magnitude that it appears possible that a study of luminescence might be made to determine points at which physical changes take place in liquids in which the dyes are dissolved, possibly including states of "association" such as are attributed to various liquids.

A Simple Stroboscope

AUSTIN J. O'LEARY, *Department of Physics, College of the City of New York*
(Received July 31, 1935)

ANY device which may be used to make objects in periodic motion appear stationary is called a stroboscope. The effect is usually accomplished by shining light intermittently on the object, the frequency of flashes being adjusted to suit the speed of motion. Detail of image is obtained by making the duration of each flash short in comparison with the interval between flashes. While individual designs are many and varied, stroboscopes have been, for the most part, of two general classes. In the one type, an electrical circuit with a very sharp potential peak is used to discharge intermittently a highly damped light source such as a spark gap, mercury vapor or neon lamp. In the other type, either the light shining upon the object or the light from the object to the eye, is interrupted mechanically.

A third method of producing the stroboscopic effect is described here in which a rotating slit of light replaces the intermittent illumination mentioned above. It is easily seen that when the light slit turns with its center of rotation coinciding with that of a rotating disk, at such a speed that it meets the same part of the disk in the same place in successive rotations, a stationary image will result. Since the light is always shining on some part of the disk, intensity of illumination is gained without loss of detail. Light from a slit parallel to the axis of rotation is used for viewing vibrating bodies such as a spring or tuning-fork. Many interesting effects are obtained which are not possible with other types of stroboscope.

CONSTRUCTION AND USE

A thirty-two candlepower, 6–8-volt, single filament automobile lamp was used as a source of light. The lamp was mounted inside a closed brass cylinder which fitted snugly into the inner ring of a roller bearing as shown in Fig. 1. An *SKF* ball bearing No. 6207A, was used; inside diameter 35 mm, outside diameter 75 mm. Electrical connection to the central contact of the lamp was made through a steel ball held against it by a spring and to the outer contact through the bearing. A slit, 1 mm wide, confined the light emerging from the cylinder to a narrow band.

A slit cut along the side of the cylinder parallel to the axis of rotation is referred to as a "side slit," one cut in the end of the cylinder along a diameter as a "diametric slit" and one cut in the end along a radius only, as a "radial slit." A diametric and side slit were combined in the one cylinder. The radial slit is mentioned only for the purpose of discussion.

A 500-watt projection lantern was also used with satisfactory results in place of the automobile lamp. A short cylinder with slit cut in the end jutted beyond one side of the bearing just far enough to permit a belt drive. The slide holder of the lantern was replaced by a wooden frame to hold the bearing and block out all the light except that coming through the slit. A sharp image of the slit was then focused on a distant rotating body.

The accessories are standard laboratory equipment, the same for either arrangement. The writer used a 1/50th horsepower, 110-volt d.c. series wound motor to rotate the light slit. An elastic band served adequately as a belt. Leads from the armature and field coil were brought out to a reversing switch, so that the motor could be run in either direction. Two rheostats of 500 and 100 ohms resistance gave a sensitive variation in speed up to 6000 r.p.m.

The speed of the motor can be measured directly with a tachometer and that of the light slit obtained from the speed ratio between the two. The speed of rotation or vibration of any other body can be measured with the stroboscope by adjusting the speed of the light slit until a stationary image is obtained since the speed ratio between the object and the light slit is known for each different image.

A photograph of the complete assembly with the automobile lamp is shown in Fig. 2(a). The intensity of illumination from this model may be gauged from the fact that exposure times of

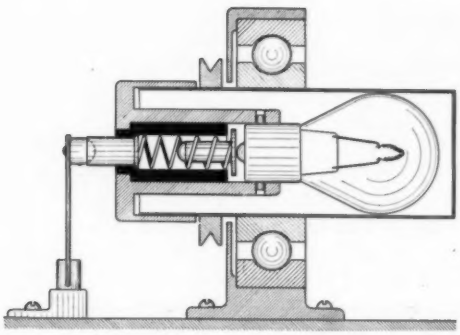

FIG. 1. Receptacle for automobile lamp.

photographs in Fig. 2 taken under its light with an f 4.5 lens and panchromatic supersensitive film, ranged from as low as 1/10 second up to no more than 4 seconds.

Typical images obtained with the stroboscope for different objects are considered under three headings.

I. Side slit

A true picture of a vibrating body such as a spring or tuning-fork may be obtained with the side slit but the image of a rotating body such as a fan is always distorted. In Fig. 2(f), the fan is rotating counterclockwise while the horizontal beam of light from the side slit is moving upward over the blades; the light slit and the fan are rotating at the same speed; if the speed ratio between the two is changed, a variety of other distorted images may be seen.

II. Diametric slit and object rotating in opposite directions

One photograph, Fig. 2(i), was taken with a radial slit and the remaining photographs of rotating bodies with a diametric slit. The light slit was rotating in the opposite direction to the object in every case.

Details regarding the images formed when the object is a disk with symmetrical vanes, are considered in the last section of this paper. Three characteristic points concerning these images are illustrated by the photographs in Fig. 2; the symbols used in the legends are explained in the last section.

(*1*) *The width of vanes in the image is always less and the number greater than in the object.*

(*2*) *Images with the same number of vanes but of a different width are sometimes obtained at several different speeds.* For example, when the object is a 4-blade fan, there are three different images, with 14 blades, see Fig. 2(j), (k) and (l). There are also three different images with 18 blades; only the widest is shown in Fig. 2 (m) with the blades overlapping. With the disk in Fig. 2(n) as object, two different images with 10 vanes are shown in Fig. 2 (o) and (p).

(*3*) *A great variety of nonsymmetrical images are produced at the different speeds when the center of rotation of the light slit is moved away from the center of the disk.* A typical one is shown in Fig. 2(h).

Like other stroboscopes the present design may be used to bring together letters on a disk to form words, and parts of a picture to form a completed picture, as in Fig. 2(t). Likewise when the disk in Fig. 2(q) is rotated, the sectors in different rings appear to rotate in opposite directions or in the same direction with different speeds. In Fig. 2(r), the disk and diametric slit are rotating at the same speed. An image is formed from each half of the slit and, at this speed, the two images coincide for an even number of sectors but are displaced for an odd number so as to form solid circles.

A unique feature is the way in which geometric patterns on a disk are transformed into figures of a different kind at various speeds of rotation as shown in Fig. 2(u), (v) and (w).

III. Diametric slit and object rotating in same direction

The images formed when the slit and disk are rotating in the same direction with different speeds are considered in detail in the section following. We consider now, effects produced when the speeds are equal.

Circular waves may be produced with the disk in Fig. 2(x). It has curved arms painted in the colors of the spectrum which appear as stationary rings when the speeds of the disk and slit are identical. If the speeds are not quite equal, the colored circles form at the center, move outward in a continuous train of waves and disappear at the rim of the disk, or *vice versa*, depending upon which speed is the greater. Another striking color effect may be produced with a disk having

(a) Stroboscope.

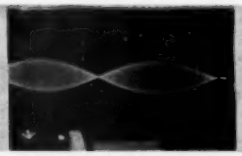

(b) Vibrating spring, ordinary illumination

(c) Same spring illuminated by side slit.

(d) Spring vibrating with 3 loops.

(e) Stationary fan. $n_o = 4$; width $= W_o$.

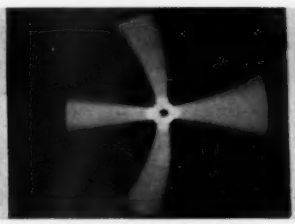

(f) Fan illuminated by side slit.

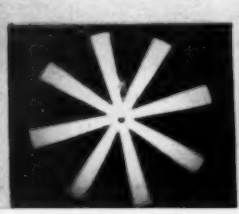

(g) $n_i = 8$; $\omega = 1$; $W_i/W_o = 1/2$.

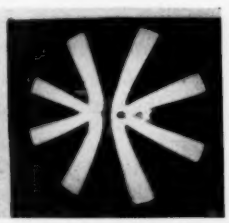

(h) Same as (g) with slit off center.

(i) $n_i = 5$; $\omega = 1/4$; $W_i/W_o = 4/5$.

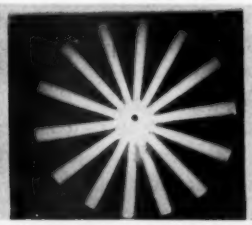

(j) $n_i = 14$; $\omega = 5/2$; $W_i/W_o = 2/7$.

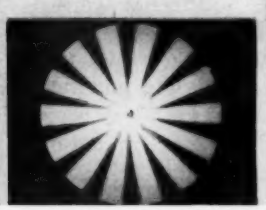

(k) $n_i = 14$; $\omega = 3/4$; $W_i/W_o = 4/7$.

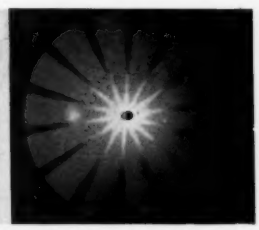

(l) $n_i = 14$; $\omega = 1/6$; $W_i/W_o = 6/7$.

(m) Image overlapping $n_i = 18$; $\omega = 1/8$; $W_i/W_o = 8/9$.

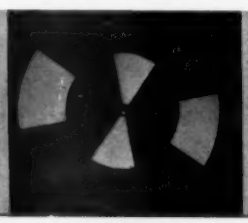

(n) Stationary disk $n_o = 2$.

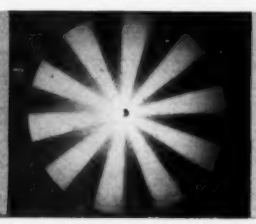

(o) Disk in (n) rotating $n_i = 10$; $\omega = 3/2$; $W_i/W_o = 2/5$.

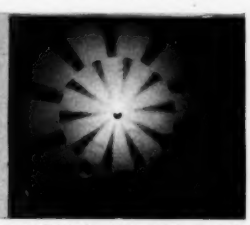

(p) Disk in (n) rotating $n_i = 10$; $\omega = 2/3$; $W_i/W_o = 3/5$.

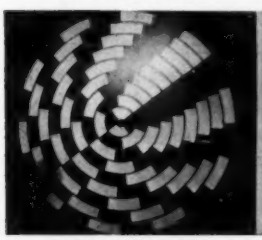

(q) Disk with sectors.

(r) Disk rotating. $\omega = 1$.

(s) Lettered disk.

(t) Disk rotating. $\omega = 1$.

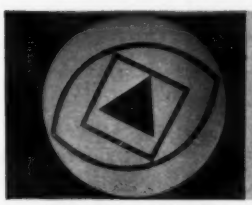

(u) Stationary disk with geometric figures.

(v) Disk in (u) rotating, $\omega = 1$.

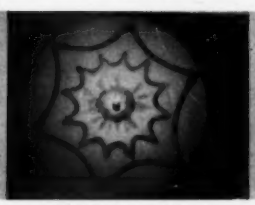

(w) Disk in (u) rotating. $\omega = 2$.

(x) Colored disk to show circular waves.

FIG. 2.

radial instead of curved arms. The disk appears to be one solid color when the speeds are equal so that the light shines all the time on the same color. As the slit and disk lag slightly behind or gain upon each other, the color of the disk changes through all the colors of the spectrum. Many interesting color patterns are obtained with each of these disks when the center of rotation of the slit is moved away from the center of the disk.

A fan appears as a solid disk when the light is shining all the time on one of the blades but when the light shines between blades the disk disappears and the motor and other objects behind the fan become visible. Similarly the disk in Fig. 2(n) appears successively, solid black, inner half black and outer half white, solid black again, then inner half white and outer half black, etc.; the disk in Fig. 2(u) shows circles of varying width which move in and out from the center; the disk in Fig. 2(q) shows circular rings alternately changing from black to white.

Images of a Disk with Symmetrical Vanes

Width

Let n_o denote the number of symmetrical vanes of width W_o on an object disk, n_i the number of vanes of width W_i appearing in a stationary image and ω, the speed ratio of the object disk to the light slit. Neglecting for a moment the width of the slit of light itself, the width of each vane in the image is just equal to the distance traveled by the light slit in passing from one side of an object vane to the other. If the two are moving in opposite directions, the light slit moves a distance W_i while the object disk moves a distance $W_o - W_i$.

$$\therefore (W_o - W_i)/W_i = \omega$$

or

$$W_i/W_o = 1/(1+\omega). \tag{1}$$

If the light slit and object disk are moving in the same direction, the light slit moves a distance W_i while the object disk moves a distance $W_i - W_o$ if $\omega<1$ and $W_i + W_o$ if $\omega>1$.

$$\therefore W_i/W_o = 1/(1-\omega) \quad \text{if} \quad \omega<1 \tag{2}$$

$$= 1/(\omega-1) \quad \text{if} \quad \omega>1. \tag{3}$$

If the angular width of each vane in an image is such that $n_iW_i<2\Pi$, each vane is separated, if $n_iW_i=2\Pi$, each vane meets to form a solid disk and if $n_iW_i>2\Pi$, the vanes overlap. When the overlapping is too great, the image becomes indistinguishable.

Detail

The effect of finite width of the light slit is to reduce the detail observable in an image by broadening each radial line on the object by an amount equal to the distance that line travels while the light is moving across it. Let B denote this broadening at any point on the disk and W_s the width of the light slit at the same point. When the slit and disk are moving in opposite directions, a radial line moves a distance, B, while the light slit moves the distance, $W_s - B$, from which we get

$$B/W_s = \omega/(1+\omega). \tag{4}$$

When the light slit and object disk are moving in the same direction, we get in a similar manner

$$B/W_s = \omega/(1-\omega) \quad \text{if} \quad \omega<1 \tag{5}$$

$$= \omega/(\omega-1) \quad \text{if} \quad \omega>1. \tag{6}$$

Intensity

Let I_o represent the intensity of illumination of the object disk when it is stationary and I_i, the intensity of illumination of an image when the disk is rotating. The amount of light reflected is proportional to the intensity of illumination times the area of reflecting surface, that is to $I_on_oW_o$ when stationary and to $I_in_iW_i$ when rotating. Since the total amount of light reflected is the same whether the disk is rotating or stationary, we have

$$I_i/I_o = n_oW_o/n_iW_i. \tag{7}$$

Speed ratio between disk and radial slit, rotating in opposite directions

The number of vanes which appear in a stationary image is determined by the speed ratio between the object and the light slit. In the case of a radial slit rotating in the opposite direction to the object disk, an image with n_i

vanes is obtained for any speed such that the light slit rotates a distance x/n_i while the object disk rotates $1/n_o - x/n_i$, where x/n_i is a fraction in its lowest terms less than $1/n_o$.

$$\therefore \omega = (1/n_o - x/n_i)/(x/n)_i$$
$$= n_i/xn_o - 1. \quad (8)$$

This is illustrated in Fig. 3(a) for the case where $n_o=3$ and $n_i=14$. The radial slit is shown meeting one of the object vanes at the point A. Dotted lines indicate the position of the image vanes. When $x=1$ or $x=3$, an image with 14 vanes is obtained which repeats itself after x rotations of the light slit. When $x=2$ or 4, $x/14$ is not in its lowest terms and the resulting image has only 7 vanes. Other examples of the application of Eq. (8) are given in Table I.

In using the stroboscope to measure speeds of rotation, we must know the particular value of ω corresponding to each image observed, that is we must know the particular value of x in case an image with the number of vanes observed is obtained at more than one speed. Combining Eqs. (1) and (8), we get

$$x = n_i W_i / n_o W_o. \quad (9)$$

Thus x is obtained from the width of the image. This is very simple when the width of vanes is such that $n_o W_o \geq \Pi$ since, in this case, all images will overlap except those for which $x=1$. For a disk painted half black and half white, $n_o=1$ and $\omega = n_i - 1$ for all images which do not overlap.

Eq. (8) also gives a unique value of n_i for any given fractional value of ω. For example, if $n_o=4$ and $\omega=1/6$, we have $n_i=14x/3$. Only the values $x=3$ and $n_i=14$ will satisfy the necessary condition that n_i be an integer and x/n_i, a fraction in its lowest terms less than $1/n_o$.

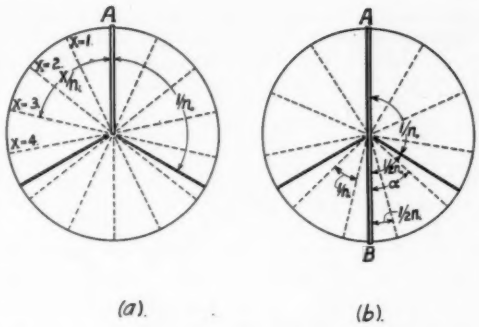

FIG. 3. (a) Illustration to show how a radial slit may meet the vanes of a disk to form images with a specified number of vanes at different speed ratios. (b) Example used in determining when the images due to the two halves of a diametric slit coincide and when they are displaced with respect to each other.

Speed ratio between disk and radial slit, rotating in the same direction

When the disk and radial slit are both rotating in the same direction, we obtain the values of ω which give an image with n_i vanes by observing that the light slit moves a distance x/n_i while the object disk moves a distance $x/n_i - 1/n_o$ if $\omega<1$ and $x/n_i + 1/n_o$ if $\omega>1$. In this case x/n_i may be any fraction in its lowest terms when $\omega>1$, and any fraction in its lowest terms greater than $1/n_o$ when $\omega<1$. We get

$$\omega = 1 - n_i/xn_o \quad \text{when} \quad \omega<1 \quad (10)$$
$$= 1 + n_i/xn_o \quad \text{when} \quad \omega>1. \quad (11)$$

As before, there is a unique value of n_i corresponding to each fractional value of ω. Some of these values are listed in Table II for the case where $n_o=4$. The table shows that when $\omega \ll 1$, W_i is always a little greater than W_o but the image is clear. When $\omega=2$, we have $n_i=n_o$ and

TABLE I. *Images having a given number of vanes, n_i, when light slit and disk are rotating in opposite directions.*

	$n_o=4$										$n_o=3$									
	Radial slit										*Radial slit*									
n_i	5	6	7	8	9	9	10	14	14	18	4	5	6	7	7	8	9	9	10	10
x	1	1	1	1	1	2	1	1	3	1	1	1	1	1	2	1	1	2	1	3
ω	1/4	1/2	3/4	1	5/4	1/8	3/2	5/2	1/6	7/2	1/3	2/3	1	4/3	1/6	5/3	2	1/2	7/3	1/9
W_i/W_o	4/5	2/3	4/7	1/2	4/9	8/9	2/5	2/7	6/7	2/9	3/4	3/5	1/2	3/7	6/7	3/8	1/3	2/3	3/10	9/10
B/W_o	1/5	1/3	3/7	1/2	5/9	1/9	3/5	5/7	1/7	7/9	1/4	2/5	1/2	4/7	1/7	5/8	2/3	1/3	7/10	1/10
	Diametric slit										*Diametric slit*									
n_i	6	8	10	10	14	14	14	18	18	18	4	5	6	7	8	9	10	12	14	16
ω	1/2	1	3/2	1/4	5/2	3/4	1/6	7/2	5/4	1/8	—	2/3	—	4/3	1/3	2	—	1	1/6	5/3
W_i/W_o	2/3	1/2	2/5	4/5	2/7	4/7	6/7	2/9	4/9	8/9	—	3/5	—	3/7	3/4	1/3	—	1/2	6/7	3/8
B/W_o	1/3	1/2	3/5	1/5	5/7	3/7	1/7	7/9	5/9	1/9	—	2/5	—	4/7	1/4	2/3	—	1/2	1/7	5/8

TABLE II. *Images corresponding to particular values of ω when light slit and disk are rotating in the same direction.*

$n_o = 4$; *Radial slit*

ω	1/6	1/5	1/4	1/3	1/2	2/3	3/4	1	4/3	3/2	2	3	4	5	6
n_i	10	16	3	8	2	4	1	—	4	2	4	8	12	16	20
x	3	5	1	3	1	3	1	—	3	1	1	1	1	1	1
W_i/W_o	6/5	5/4	4/3	3/2	2	3	4	∞	3	2	1	1/2	1/3	1/4	1/5
B/W_o	1/5	1/4	1/3	1/2	1	2	3	∞	4	3	2	3/2	4/3	5/4	6/5

$W_i = W_o$ so that image and object are identical; however, at this speed, $B/W_o = 2$, so that detail is poor except for a very narrow slit. When $\omega \gg 1$, each image is almost as sharp and as narrow as when disk and light slit are rotating in opposite directions; thus the speed of rapidly rotating bodies may also be measured in this way. The appropriate value of x corresponding to any observed image is again determined by the width of the image according to Eq. (9), as may be seen by combining Eqs. (2) and (10) and Eqs. (3) and (11), respectively. For a disk painted half black and half white, $\omega = n_i + 1$ for each image which does not overlap.

Speed ratio between disk and diametric slit

In the case of every image with the radial slit where n_o and n_i are both even or where n_o, n_i and x are odd, an identical image is obtained at the same speed with the diametric slit due to the coincidence of the image from each half of the slit. In the case of all other images with the radial slit, an image with twice as many vanes of the same width is obtained at the same speed with the diametric slit since each vane in the image from one-half, falls midway between the vanes in the image from the other half of the slit. As an illustration let us consider only one case, namely that for which n_o and n_i are both odd and the disk and light slit are moving in opposite directions. Suppose the upper part of the light slit coincides with one of the vanes of the disk at the point A, Fig. 3(b). The lower part of the diametric slit will be, at that instant, at the point B. If we let α be the distance it travels before meeting the next vane, separated from it by the distance $1/2n_o$, we have

$$\omega = (1/2n_o - \alpha)/\alpha,$$
$$\alpha = 1/2n_o/(1+\omega)$$
$$= x/2n_i \text{ from Eq. (8).}$$

From this it is seen that the lower part of the slit will meet a vane of the disk along one of the dotted lines coincident with the image from the upper half when x is odd but when x is even will meet the vane midway between two of the dotted lines and give an image with twice as many vanes of the same width as with the radial slit. The other cases are treated in a similar manner with the result already stated. Thus, for any particular value of ω, the corresponding value of n_i with the diametric slit is easily found from the value of n_i with the radial slit.

When it is desired to know all values of ω which give an image with n_i vanes with the diametric slit, the following rules may be applied.

1. A disk with n_o even.
   (a) n_i odd—not possible.
   (b) n_i even, $n_i/2$ even—same as for n_i vanes with the radial slit.
   (c) n_i even, $n_i/2$ odd—same as for both n_i and $n_i/2$ with the radial slit.
2. A disk with n_o odd.
   (a) n_i odd—same as for n_i vanes, x odd, with the radial slit.
   (b) n_i even, $n_i/2$ odd—same as for $n_i/2$ vanes, x even, with the radial slit.
   (c) n_i even, $n_i/2$ even—same as for $n_i/2$ vanes with the radial slit.

These rules apply whether the disk and light slit are rotating in the same or the opposite direction. Their application is illustrated by the set of values given in Table I.

In conclusion, the writer is pleased to express his appreciation to Messrs. George Kayser and Vladimir Gorshkoff for their skillful mechanical work.